New Treatment Opportunity for Acute Myeloid Leukemias Harbouring a *UBTF* Tandem Duplication

Rebecca Mohnani

August 2023

A Research Project Presented to the Faculty of Medicine for the Degree of Master of Science in Biomedical Science at Utrecht University.

Institute: Princess Máxima Center for Pediatric Oncology
Principal Investigator: Olaf Heidenreich
Daily Supervisor: Milad Rasouli

Abstract

Tandem duplications in the upstream binding transcription factor (*UBTF*-TD) have been recently identified as a recurrent mutation in pediatric acute myeloid leukemia (AML). They are seen in 4% of *de novo* patients and 9% of relapse cases. Transcriptionally similar AML subtypes, such as *MLL*-rearranged, *NUP98*- rearranged, and *NPMI*-mutant AMLs, were found to respond to small molecular inhibitors to the menin-MLL1 interaction which is critical for leukemogenesis. We hypothesized that due to similarities in the oncogenic programs of these AML subtypes with AMLs harboring the *UBTF*-TD alteration, implementation of Menin inhibitors could lead to a reduction in the leukemic characteristic of *UBTF*-TD AMLs. This hypothesis was tested by treating primary *UBTF*-TD AML cells with the Menin inhibitor SNDX-5613 (Revumenib) and looking at its effect on global gene expression via RT-qPCR and RNA sequencing. Since *UBTF*-TD AMLs are often accompanied by *FLT3*-ITDs, we also looked at the effect of SNDX-5613 and its combination with an FLT3 inhibitor on this protein through phopho-STAT5 signaling pathway analysis. We found that Menin inhibition substantially changed global gene expression of *UBTF*-TD AMLs, including downregulation of important downstream target genes that depend upon the Menin-MLL interaction and upregulation of differentiation markers. Phospho-STAT5 signaling analyzed by flow cytometry revealed that individual treatment was as effective (Gilteritinib) or more effective (SNDX-5613) than combination treatment.

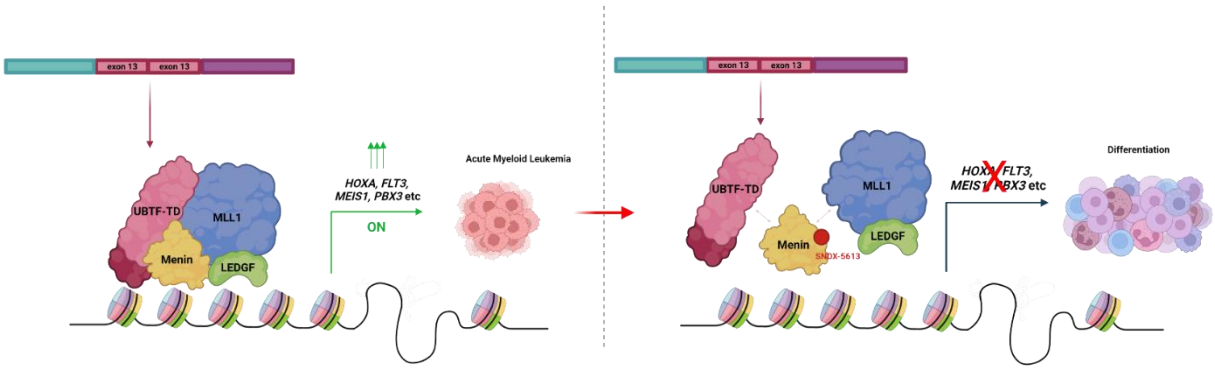

A proposed visual representation of the interaction of Menin-MLL1 and UBTF-TD and the effect of treatment with SNDX-5613.

Created with BioRender.com

Plain Language Summary

Leukemias are cancers of early blood-forming cells and tissues and are most often seen in the white blood cells. They can be divided into multiple subcategories based on the type of cells being affected and the mutation that is causing the pathology. My project focuses on a leukemia subtype in children called acute myeloid leukemia (AML) characterized by a mutation called an upstream binding transcription factors tandem duplication (*UBTF*-TD). This mutation has recently been found to be more common in childhood AML than previously thought, and its association with poor survival rates means that there is need for an effective treatment to be found. Previous research has shown that *UBTF*-TD AMLs are genetically similar to some other AML subtypes. This means that therapies that have been successful for these AML subtypes may also work for the newly identified *UBTF*-TD AML subtype.

This research project focuses on the drug SNDX-5613 which targets a protein called Menin. Menin is thought to be critical for the mechanism that drives *UBTF*-TD AML, so if it can be blocked by SNDX-5613, we hypothesize that the leukemia will be suppressed. In this project, the effect of this drug (SNDX-5613) was tested by treating cells taken directly from pediatric patients. Using techniques termed RT-qPCR and RNA sequencing we then looked at which genes have been affected following treatment, and how they differ when compared to the untreated samples. We found that following treatment, key genes that play a role in the onset and maintenance of leukemia were decreased in production.

We then specifically looked at a gene called fms-like tyrosine kinase 3 (*FLT3*) which is often mutated in *UBTF*-TD AMLs. When mutated, this gene may play a role in increased cancerous cell counts; so, any reductions observed following treatment could be linked to improvements of the treated illness. In AML, FLT3 may take at least 4 different forms, meaning that it could be difficult to detect one form only and get accurate results. Mutations in *FLT3* (*FLT3*-ITDs) lead to the activation of the phospho-STAT5 signaling pathway, meaning that any changes in phospho-STAT5 would be directly proportional to changes in *FLT3*-ITD. We therefore looked at phospho-STAT5 expression following

treatment with SNDX-5613. This revealed a reduction in pSTAT5 production, and thus in FLT3-*ITD* similarly.

Previous research has shown that the combination of a drug targeting Menin, like SNDX-5613, and a drug that targets FLT3, like Gilteritinib, may work together to have an effect that is greater than the sum of their effects separately. Therefore, we set out to test this on patient samples that have the *UBTF*-TD mutation. Once again we looked at phospho-STAT5 and saw that although both SNDX-5613 and Gilteritinib are able to separately decrease the production of phospho-STAT5 and FLT3, when combined, no cooperative effect is seen.

Chapter 1 – Introduction

1.1 Acute Myeloid Leukemia

Leukemia refers to a group of hematologic cancers that arise from the malignant transformation of haematopoietic stem and progenitor cells (Hoffbrand, Steensma 2020). Acute myeloid leukemia (AML) is defined by the accumulation of ≥20% early myeloid bone marrow progenitors in the bone marrow or peripheral blood, resulting in insufficient erythropoiesis and eventual bone marrow failure. AML is the most common leukemia in adults but is rarer in children. As modern medicine continues to evolve, patient outcomes have improved to 70% overall survival (OS) in children, while cure rates for patients below and above 60 years of age stands around 40% and 15%, respectively (Vakiti, Mewawalla 2023, de Rooij -, Zwaan et al. 2015).

Mutations in hematopoiesis-related genes might give rise to AML, but the underlying cause remains undetermined. AML is a highly heterogenous cancer with variable prognoses, and the pathophysiology involves two cooperating genetic events: type I mutations result in reduced cellular apoptosis and increased proliferation through abnormalities in signal transduction pathway genes such as *FLT3, N-RAS,* and *PTPN11,* and type II mutations involve genetic abnormalities in hematopoietic transcription factors resulting in hindered differentiation (de Rooij -, Zwaan et al. 2015). The molecular landscape in pediatric AML is significantly distinct from that in adult AML. Translocations contribute predominantly in pediatric AML and give rise to abnormal transcription and gene expression caused by the fusion protein itself or co-factor recruitment to the respective transcription complex. The most common pediatric cytogenetic abnormalities are t(8;21)(q22;q22), inv(16)(p13.1q22) (CBF-AML), t(15;17)(q22;q21), and 11q23/*MLL*-rearranged AMLs (de Rooij -, Zwaan et al. 2015).

The current treatment approach for pediatric AML involves intensification of induction chemotherapy (combination of cytarabine and anthracycline), followed by consolidation chemotherapy. Although intensive, this treatment regime results in relapse in ~30% of patients (Vakiti, Mewawalla 2023, de Rooij -, Zwaan et al. 2015). Treatment-related deaths and long-term side effects, such as anthracycline-induced cardiomyopathy and lung damage, indicate that further intensification of

chemotherapy is no longer an option (de Rooij -, Zwaan et al. 2015, Slats, Egeler et al. 2005). As a result, the development of more effective, safer, and less damaging molecularly targeted therapies is needed.

1.2 Upstream Binding Transcription Factor Tandem Duplication (*UBTF*-TD)

The upstream binding transcription factor (*UBTF*) gene is located at the long arm of chromosome 17 (17q21) and encodes a nucleolar protein that functions in mRNA transcription regulation via RNA polymerase I or II. Alterations in *UBTF* are closely linked with childhood neurodegeneration and cancers such as melanoma, lung and colon cancers, and acute lymphoblastic leukemia (ALL) (Duployez, Vasseur et al. 2023). Recently, tandem duplications (TDs) in the *UBTF* gene involving exon 13 have been identified as a recurrent mutation in pediatric acute myeloid leukemia (AML), as a subtype that previously had no known oncogenic driver (Umeda, Ma et al. 2022).

UBTF-TDs account for 4% of pediatric AMLs at diagnosis and 9% of relapse cases, and often present with trisomy 8, *FLT3*-internal tandem duplications (*FLT3*-ITDs) and *WT1* mutations. AML patients with *UBTF*-TDs are associated with a poor prognosis, dismal outcome, and minimal residual disease (MRD) positivity following induction chemotherapy (Kaburagi, Shiba et al. 2023, Umeda, Ma et al. 2022). Research has also shown that *UBTF*-TD is mutually exclusive with other AML subtype-defining genetic alterations and induces distinct transcriptional programs similar to *NUP98*-r and *NPM1* AMLs, including elevated expression of *HOX/MEIS1* genes (Umeda, Ma et al. 2022).

Figure 1.1 **- *UBTF* gene structure and location of *UBTF*-TDs**

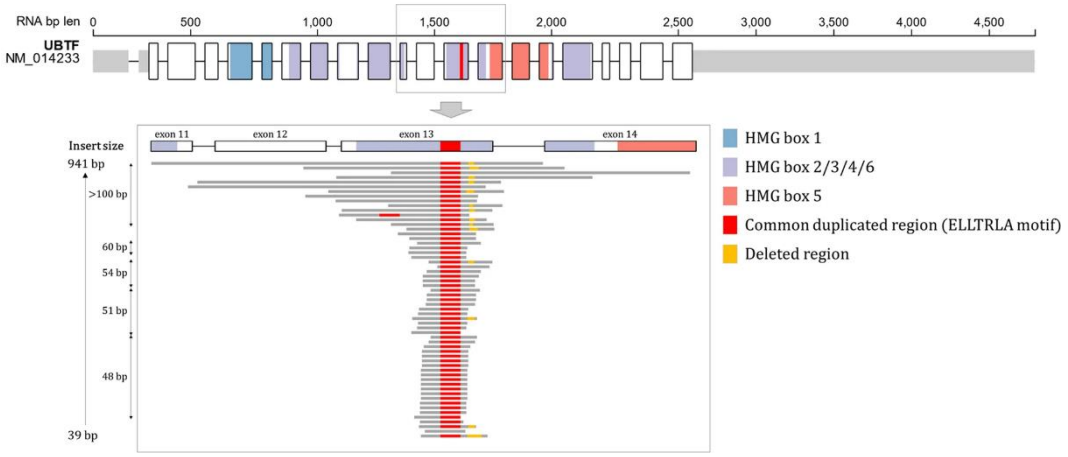

Tandem duplications (TDs) of the *UBTF* gene involving exon 13, seen in the figure above, have been identified as a recurrent mutation in pediatric acute myeloid leukemia (AML).

(Duployez, Vasseur et al. 2023)

1.3 FMS-like Tyrosine Kinase 3 (FLT3)

FMS-like tyrosine kinase 3 (FLT3) belongs to the class III receptor tyrosine kinase family, and plays a crucial role in hematopoietic proliferation, differentiation, and survival (Lagunas-Rangel, Chávez-Valencia 2017, Takahashi 2011). Changes in the *FLT3* gene involve two main types of alterations. One is a point mutation in exon 20, referred to as FLT3-TKD, which results in a missense mutation in the FLT3 activation loop. The other, more commonly observed alteration, is the internal tandem duplication (ITD) in the FLT3 juxtamembrane (JM) domain, occurring in exons 14 and 15 (Lagunas-Rangel, Chávez-Valencia 2017). This ITD has been linked to a poor prognosis due to the resultant constitutive ligand-free activation of FLT3 kinase via loss of autoinhibitory functions. This activates downstream proliferative signaling pathways, including the Ras/MAPK kinase (MEK)/ extracellular signal-regulated kinase (ERK) pathway, the PI3K/Akt pathway, and interestingly the STAT5 pathway which is not seen in wild-type FLT3 signaling. Activation of the latter directly contributes to leukemogenesis via the induction of STAT5 target genes like cyclin D1, c-myc, and p21, all needed for cell growth (Lagunas-Rangel, Chávez-Valencia 2017). *FLT3*-ITDs have also been found to

activate Pim serine threonine kinases which may also lend a hand in malignant behavior (Takahashi 2011). Such mutations may accelerate the production of reactive oxygen species (ROS) through STAT5 mediated RAC1 activation and $p22^{phox}$ and NOX4 activation, leading to faulty repair mechanisms and more DNA double-strand breaks (DSBs) (Lagunas-Rangel, Chávez-Valencia 2017).

Figure 1.2 **– *FLT3*-ITD Mediated Activation of STAT5**

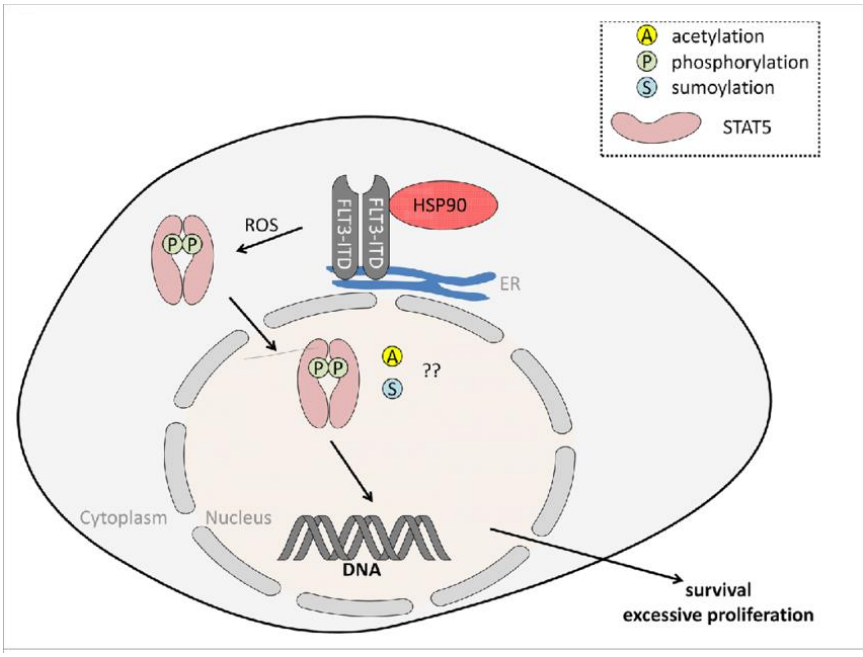

FLT3-ITDs lead to the activation of aberrant signaling and direct phosphorylation of STAT5 in an SFK- and JAK-independent manner, leading to excessive cell proliferation.

(Kosan, Ginter et al. 2013)

1.4 Menin and the Menin-MLL Interaction

Menin, a primarily nuclear protein encoded by the *MEN1* gene, is expressed ubiquitously. Its functions are tissue specific, as demonstrated by its ability to act as a tumor suppressor in the endocrine organs but has an antagonistically critical role in leukemogenesis (Yokoyama, Somervaille et al. 2005). These seemingly opposing functions may be due to Menin's ability to regulate gene expression both positively and negatively through its interaction with a variety of other proteins, of which the transcription activator MLL1 is of particular interest in the context of AML. It has been documented

that Menin plays a vital role in the development of *MLL*-r AML, where MLL1, an enzyme involved in chromatin modification, carries out histone methyltransferase (HMT) activity, leading to the methylation of histone H3 at lysine 4 (H3K4me3). This process maintains the chromatin in an activated state. The interaction between Menin and MLL has also been identified as a critical molecular dependency in other AML subtypes such as *NUP98*-r and *NPM1* mutant AMLs (Yokoyama, Somervaille et al. 2005).

In general, Menin recruits MLL protein complex to the gene loci of critical leukemic genes like *HOXA9* and *MEIS1*, where they make a critical interaction via the N-terminal of MLL and induce open active chromatin (Matkar, Thiel et al. 2013).

Figure 1.3 **– The four classes of proteins that interact with Menin**

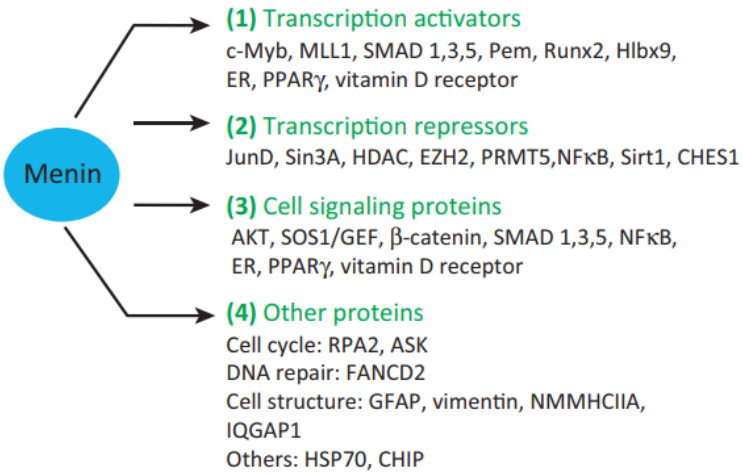

The proteins that interact with Menin may be grouped into four major categories based upon their relative functions. The transcription activator MLL1 is of importance for AML.

(Matkar, Thiel et al. 2013)

FLT3 inhibitors have seen some success in reducing leukemic burden via cell-cycle arrest, proliferation hindrance, and induced apoptosis, but the clinical efficacy of single treatment is insubstantial (Dzama, Steiner et al. 2020). Research has shown possible synergistic effects between FLT3 inhibitors and Menin-MLL inhibitors in *MLL*-r and *NPMI*^{mut} leukemias through the downregulation of *MEIS1* via Menin-MLL inhibitors leading to the inhibition of its putative transcriptional target gene, *FLT3*. This is enhanced by FLT3 inhibitors which have on-target anti-pFLT3 effects (Dzama, Steiner et al. 2020).

1.5 Small Molecular Inhibitors: SNDX-5613

This idiosyncrasy of having a biochemical interaction between a tumor suppressor protein (Menin) and a protooncogenic protein (MLL) led to the discovery that MLL oncoproteins rely critically on Menin to maintain leukemic behavior (Yokoyama, Somervaille et al. 2005). As a result, small molecular Menin inhibitors have been developed, which function by suppressing downstream targets that depend upon the Menin-MLL1 interaction. Structural studies of Menin have revealed the site of protein-protein binding with MLL as a highly suitable target for small molecular inhibitors. This central cavity binds with two short motifs within the N-terminus of MLL: Menin binding motif 1 (MBM1, K_d = 56nM), and menin binding motif 2 (MBM2, K_d = 1µM). Blocking the pocket of both binding motifs is not feasible, and albeit, it was found that the sole blocking of the MBM1 binding site is sufficient to disrupt the interaction between Menin and MLL effectively (Cierpicki, Grembecka 2014).

An example of a menin inhibitor, and the one being used for this project, is SNDX-5613 which is also termed revumenib. Revumenib has already been used in the early-phase clinical trial AUGMENT-101. Following treatment, 18 patients experienced complete remission and 12 patients were able to receive a stem cell transplant following remission (Reynolds 2023). Some patients developed quick resistance to Revumenib due to responsive mutations in the *MEN1* gene, but the possibility of combination therapy gives a hopeful outlook. Success will be greatly impactful as Menin is predicted to play a role

in 40-50% of all AMLs, potentially including *UBTF*-TD AMLs as is being investigated in this project (Reynolds 2023, Issa, Aldoss et al. 2022).

Figure 1.4 **– The effect of Revumenib on the Menin-MLL1 interaction**

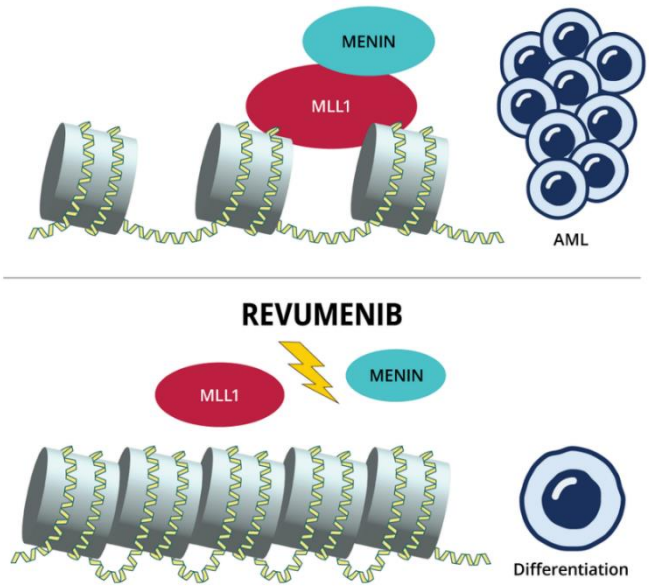

Revumenib disturbs the Menin-MLL1 interaction, leading to reduced aberrant gene expression and thus promotes cell differentiation.

(Reynolds 2023)

1.6 Direct Cell Co-Culture

Throughout this project, *UBTF*-TD AML cells were cultured onto mesenchymal stromal cells (MSCs) in a system termed direct cell co-culture. In this method, two types of cells, the tumor cells and the stromal cells, are in direct physical contact with each other in a single compartment, creating a system that resembles the *in vivo* tumor microenvironment. The effect of the stromal cells on the leukemia cells, and vice versa, may be analyzed in this way (Syama, Hassan et al. 2021). The hematopoietic bone marrow microenvironment plays a significant role in hematopoietic stem cell (HSC) generation, self-renewal, growth, and differentiation (Konopleva, Konoplev et al. 2002, Brenner, Nepstad et al. 2017). This is carried out through the MSC secretion of HSC-supporting factors such as stem cell

factor (SCF), C-X-C motif chemokine ligand 12 (CXCL12), and angiopoietin, as well as through molecular signals like CXCL12-mediated CXCR4 signaling and Wnt-induced β-catenin signaling (Tan, Kan et al. 2022, Ito, Barrett et al. 2015).

Through similar signals, the leukemic stem cell (LSC) niche has been found to support the maintenance and progression of leukemia. This crosstalk may have significant implications in the protection of residual leukemic cells from chemotherapeutic agents through the release of soluble mediators (Konopleva, Konoplev et al. 2002, Brenner, Nepstad et al. 2017). This highlights the importance of considering stromal cell-mediated chemoresistance when testing new therapeutic agents, for which cell co-culture is a viable opportunity. These abovementioned points and the supportive antiapoptotic and proliferative effects of MSCs on AML cells make direct cell co-culture a suitable system for the aim of this project (Brenner, Nepstad et al. 2017).

Chapter 2 - Materials and Methods

2.1 Sample Collection and Preparation

This project focused particularly on acute myeloid leukaemia (AML) defined by an upstream binding transcription factor tandem duplication (*UBTF*-TD). Patient samples harboring *UBTF*-TD were provided by Prinses Maxima Centrum for Pediatric Oncology after written informed consent was given. The genetic profile of all used patient samples revealed concomitant *FLT3*-ITD and *WT1* somatic mutations. The samples collected from these patients were either peripheral blood samples or bone marrow aspirations which were frozen in liquid nitrogen following collection. Samples were obtained following a request to the Prinses Máxima Center's biobank under the approved experiment number belonging to Milad Rasouli as part of his PhD project.

2.2 Primary Cell Co-Culture

In this study, we employed a mesenchymal stem cell (MSC) co-culture platform to culture patient-derived AML cells. This platform involves placing AML cells next to MSCs, aiming to retain the supportive effects of MSCs on AML cells and mimic the *in vivo* tumor microenvironment. Each part of cell co-culture involves particular cell culture media that function to nourish the cells allowing for growth and reduced apoptosis.

Healthy bone marrow-derived MSCs were cultured in Dulbecco's Modified Eagle Medium (DMEM) (1x), low glucose + GluctaMAX™ Supplement, pyruvate (ThermoFisher Scientific, Waltham, MA), supplemented with 20% fetal bovine serum (FBS), 100µ/mL Pen-Strep (P/S) (Gibco BRL, Life Technologies, Breda, The Netherlands), and 8ng/ml basic fibroblast growth factor (b-FGF) (FGF2; PeproTech, London, UK) and incubated at 37°C in 5% CO_2 overnight or until reaching 50-70% confluency.

When MSCs arrived to 50-70% confluency, primary AML cells were thawed and seeded on the MSC layer at a density of $5x10^5$ cells/mL in StemSpan™ Serum-Free Expansion Medium (SFEMII) (STEMCELL Technologies, Cologne, Germany). This medium was supplemented with the following cytokines. Co-cultures were expanded with adjusting AML cell numbers every 4 days.

Component	Concentration	Supplier
IL-3 (interleukin-3)	10 ng/mL	Peprotech
GM-CSF (granulocyte-macrophage colony-stimulating factor)	10 ng/mL	Peprotech
FL3-L	10 ng/mL	Peprotech
SR1 (Stem Regenin 1)	750 nM	Biogene, Lausanne, Switzerland
UM729	1.35 μM	StemCell Technologies, Cologne, Germany
SCF (stem cell factor)	150 ng/mL	Peprotech
TPO (thrombopoietin)	100 ng/mL	Peprotech
P/S (Pen-Strep)	100 μ/mL	Gibco BRL, Life Technologies, Breda, The Netherlands

2.3 Inhibitor Treatment

Primary AML cells were thawed, plated onto pre-seeded MSCs, and kept in co-culture for 3-4 days. This was followed by cell replating on fresh MSCs and treatment with 250nM SNDX or 0.1% DMSO (mock). Manual cell counts were carried out followed harvesting (see below) for accurate adjustment of AML cell concentration to 5×10^5 cells. These cells were replated and treated in 3-4 day increments for a standard of 14 days; however, this timeline differed based on experiment variations and specifications. For Gilteritinib treatment, primary AML cells were placed in co-culture for 7 days with passaging and medium refreshment in between, then treated with 10nM, 100nM, and 1000nM Gilteritinib followed by harvesting 30 minutes and 2 hours after treatment. Combination treatment was carried out by putting primary AML cells in co-culture for 7 days with concomitant SNDX-5613

(250nM) 0.1% DMSO (mock) replenishment, then treating cells with 100nM Gilteritinib and harvesting cells after 2 hours.

2.4 Cell Line Culture

Cells lines were cultured in Roswell Park Memorial Institute (RPMI) 1640 Medium (1X) + GluctaMAX™-l (ThermoFisherScientific). This medium was supplemented with 10% FBS and 100 µ/mL P/S (Gibco BRL, Life Technologies, Breda, The Netherlands). Cell lines used included: MV4-11, RL048, and Kasumi-1 cells. Cell line cultures were maintained at 37°C in 5% CO_2. Cell lines were treated with 25nM/250nM SNDX-5613 or 0.1% DMSO every 4 days with appropriate passaging and refreshing of medium in between, maintaining a cell concentration of 5 x 10^5 cells/ml.

2.5 Manual Cell Count

10µl Trypan Blue Solution, 0.4% (ThermoFisher Scientific) was pipetted into a suitable well. Trypan Blue has a negatively charged chromophore which can only react intracellularly if the cell membrane is damaged, so dead cells can take up such a stain but viable cells are unable to. This allows for differentiation between the two based on microscopic cell appearance when using a haemocytometer and an appropriate filter. 10µl of our cell suspension was pipetted into the same well and mixed with the Trypan Blue Solution. A clean haemocytometer was covered with a cover slip and 10µl of the stained, diluted cell suspension was applied to the surface of the haemocytometer at the edge of the coverslip. Each chamber was allowed to fill by capillary action. The haemocytometer was placed on the stage of a light microscope and the cells present in the four outside squares of the haemocytometer were counted.

2.6 Fluorescence-Activated Cell Sorting (FACS)

On day 7 and day 12 of treatment, co-cultures were harvested and sorted using fluorescence-activated cell sorting (FACS). This was done in order to separate our treated AML cells from the MSCs used for co-culture. For FACS sorting, primary human AML cells were harvested, washed, and suspended in PBS with 1% FBS, followed by antibody staining.

Antibody	Clone and Dilution	Target/ Function
Brilliant Violet 421 Anti-Human CD73	Clone AD2, dilution 1:20	MSCs
APC Anti-Human CD33	Clone P67.6, dilution 1:25	AML cells
APC Anti-Human CD45	Clone: HI30, dilution 1:25	AML cells
Human IgG	-	To prevent nanospecific binding of antibodies to other proteins

Unstained cells were used for defining gating strategy, using SONY Cell Sorter SH8005. AML cells were sorted based on $CD45CD33^{+}$ markers and exclusion of MSCs was carried out based on the $CD73^{+}$ marker. Post-sorting analysis was then carried out on sorted cells to ensure high quality sorting; satisfactory results of around 5% MSC contamination were obtained. Finally, cells were lysed by the addition of 350µl Buffer RLT Lysis Buffer (QIAGEN), and the final cell suspensions were transferred into adequately labelled 1ml Eppendorf tubes and placed in the -70^{o}C freezer.

2.7 RNA Extraction

RNA extraction was carried out using the Nucleospin® RNA kit (Macherey-Nagel, Düren, Germany), and RNA extractions were performed according to manufacturer's instructions. This protocol was carried out on the mock and SNDX-5613 sorted material from treatment day 7 and day 12 of patients 1, 2 and 3. Prior to methodology initiation, it was ensured that the pipettes and the hood were cleaned

using RNase*Zap*™ RNase Decontamination Solution (ThermoFisher Scientific) together with the general cleaning protocol. All tubes were labelled appropriately and stored in the -70ºC freezer.

2.8 RNA Quantification

2.8.1 RNA Quantification Using NanoDrop Spectrophotometry

NanoDrop Spectrophotometry was used to give an indication of yield. Following the addition of 1µl of RNase-free water to blank the machine, 1µl of diluted extracted RNA of the mock and SNDX-5613 samples was added. Both tubes were then labelled appropriately and stored in the -70ºC freezer once again.

2.8.2 RNA Quantification Using Qubit™ (ThermoFisher Scientific)

RNA concentrations were measure by Qubit™ RNA HS Assay Kit (ThermoFisher Scientific) (LOT: 2462687) according to manufacturer's instructions. Since Qubit™ is very sensitive, and in order to have the RNA amount within detectable range, we diluted RNA samples by at least 1:10. Our samples and their sorted cell counts were as follows:

1	Patient 1_d7 Mock	1 x 10^6 sorted cells
2	Patient 1_d7 SNDX	1.2 x 10^6 sorted cells
3	Patient 2_d7 Mock	1.2 x 10^6 sorted cells
4	Patient 2_d7 SNDX	1.9 x 10^6 sorted cells
5	Patient 1_d12 Mock	1.2 x 10^6 sorted cells
6	Patient 1_d12 SNDX	2.3 x 10^6 sorted cells
7	Patient 2_d12 Mock	0.35 x 10^6 sorted cells
8	Patient 2_d12 SNDX	1.2 x 10^6 sorted cells
9	Patient 3_d12 Mock	2 x 10^6 sorted cells
10	Patient 3_d12 SNDX	0.6 x 10^6 sorted cells
11	Patient 3_d7 Mock	2 x 10^6 sorted cells
12	Patient 3_d7 SNDX	0.7 x 10^6 sorted cells

2.9 RNA Quality Check using Agilent RNA 6000 Nano Reagents (Santa Clara, CA)

This protocol required ≥25 ng/µl RNA; for samples with less RNA the original, undiluted RNA source was used. Once again, the protocol was carried out according to manufacturer's instructions. The gel-dye mix was prepared and loaded. A new RNA chip was placed onto the chip priming station and all wells were pipetted appropriately. The ladder and samples were then pipetted. The chip was placed horizontally in the IKA vortexer, vortexed, then run in the Agilent 2100 Bioanalyser Instrument (Agilent Technologies, Santa Clara, CA, USA) using the assay class: Eukaryote Total RNA Nano within 5 minutes.

2.10 cDNA Synthesis

Synthesis of the first strand of cDNA from extracted RNA was carried out using the RevertAid™ H Minus First Strand cDNA Synthesis Kit (ThermoFisher Scientific). RevertAid Reverse Transcriptase (RT) is utilized in this kit for the synthesis of cDNA (complementary DNA).

First strand cDNA synthesis was initiated by thawing, mixing, and briefly centrifuging the components of the kit, and then storing them on ice. In the indicated order, the following reagents were then added into sterile, nuclease-free tubes on ice: the respective volume of RNase-free water, 1µl R-primer (Random Hexamer Primer, LOT 01144488), and the respective volume of RNA (shown below). The strips were vortexed, spun down, and then loaded into the Thermal Cycler PCR.

	Sample	Qubit™ Result	RNA (µl)	R-primer (µl)	RNase-free H_2O (µl)
1	Patient 1-d7-Mock	546	0.92	1	10.08
2	Patient 1-d7-SNDX	566	0.88	1	10.12
3	Patient 2-d7-Mock	450	1.11	1	9.89
4	Patient 2-d7-SNDX	488	1.02	1	9.98
5	Patient 1-d12-Mock	476	1.05	1	9.95
6	Patient 1-d12-SNDX	598	0.84	1	10.16
7	Patient 2-d12-Mock	66	7.58	1	3.42
8	Patient 2-d12-SNDX	336	1.49	1	9.51
9	Patient 3-d12-Mock	276	1.81	1	9.19
10	Patient 3-d12-SNDX	97	5.15	1	5.85
11	Patient 3-d7-Mock	314	1.59	1	9.41
12	Patient 3-d7-SNDX	165	3.03	1	7.97

In the meantime, the Master mix was prepared. The following components were added per sample in the indicated order: 4 µL 5X Reaction Buffer for RT (LOT 01046058), 1 µL RiboLock RNase Inhibitor (20 U/µL) (LOT 01153343), 2 µL 10mM dNTP Mix (LOT 01143749), and 1 µL RevertAid H Minus Reverse Transcriptase (200 U/µL) (LOT 01122843). Master mix was added after 6 minutes of PCR (when at 25^{o}C for 10 minutes). After PCR was completed, 80µl of water was added to each tube to dilute the cDNA sample. The samples were stored in the -70^{o}C freezer.

2.11 Reverse-Transcriptase Quantitative Polymerase Chain Reaction (RT-qPCR)

Reverse transcriptase quantitative polymerase chain reaction (RT-qPCR) was carried using SsoAdvanced™ Universal SYBR® Green Supermix (Bio-Rad). Thermal cycling conditions were initiated at 95°C for 30 seconds, followed by 35 cycles at 95°C for 15 seconds and 60°C for 30 seconds. RT-qPCR was carried out in triplicates and run on Bio-RAD CFX384 Real-Time System CT029144 (384W) (Bio-Rad Laboratories, California).

Primers were designed using Thembi Primer-BLAST tool and were as follows:

Gene	Forward Primer Sequence	Reverse Primer Sequence	Product Size (bp)
MEIS1	ACAGCAGTGAGCAAGGTGAT	TTGGGAAAGATGCCACGCTT	115
FLT3	GCAATTTAGGTATGAAAGCCAGC	CTTTCAGCATTTTGACGGCAACC	238
PBX3	GAGCTGGCCAAGAAATGCAG	GGGCGAATTGGTCTGGTTG	249
MEF2C	TCCACCAGGCAGCAAGAATACG	GGAGTTGCTACGGAAACCACTG	102
CDK6	CGGAGAACACCCTTGGTGG	TAGGCGGTTTCCTTGGAGAAG	128
HOXA9	GCTTGTGGTTCTCCTCCAGT	GTTGGCTGCTGGGTTATTGG	126
IGF2BP2	GTTGGTGCCATCATCGGAAAGG	TGGATGGTGACAGGCTTCTCTG	122
CD11b	TAACATCACCAACGGAGCCC	TTTCTCACTGCGGAAGGCAT	169
MDNA	CATCGGAAGCAAGAGGGAGG	ATGAGGTCTGGGGTAGTGGG	171

RNase-free water, SYBR green, and the corresponding primers were added to the plates, followed by diluted cDNA and Master mix. Measurements were expressed as Cycles to Threshold (Ct), and fold change relative to the control condition was calculated by the comparative ΔΔ cycle threshold method using TBP as the housekeeping gene for normalization.

2.13 Flow Cytometry

The effect of SNDX-5613 and Gilteritinib was characterized by flow cytometry using PE anti-STAT5 Phospho (Tyr694) Antibody - Clone: A17016B.Rec (LOT: B309312).

For flow cytometry preparation, the following reagents were needed and prepared:

- Cell staining buffer (FACS buffer): 0.5% BSA and 0.05% Sodium Azide (NaN_3) was added to PBS.
- Fixation Buffer: 4% paraformaldehyde in PBS.
- Permeabilization buffer: for the preparation of 10ml, 30µl Triton™ X-100 (Sigma-Aldrich) was added to 10ml FACS buffer. This was stored at 4ºC.

Co-cultured cells were harvested, washed, and treated with 10 µl ViaKrome 808 Fixable Viability dye (Beckman Coulter, Life Sciences) in 1000 µl PBS. Cells were washed and treated with 100µl 4%

formaldehyde per 1 million cells. Following appropriate washing and incubating steps with FACS buffer and permeabilization buffer, 50µl Permeabilization Buffer, 2.5µl Human IgG, and 1µl PE anti-STAT5 Phospho (Tyr694) Antibody - Clone: A17016B.Rec (LOT: B309312) were added per well, omitting the antibody in unstained wells. Further washing with permeabilization was followed by FACS carried out on CytoFLEX LX Flow Cytometer (Beckman Coulter).

2.14 Bulk RNA-Seq

For gene expression analysis, reads were mapped to the human genome (Hg38) using STAR (v2.2.0c). Only reads that mapped to unique genomic locations (MAPQ > 10) were used for downstream analysis and differentially expressed genes between the treated groups were identified using DESeq version 2.

Chapter 3 - Results

3.1 Overview of Results

In this section, the key findings and relevant results obtained that pertain to the specific aims and objectives of this research project will be presented. The first set of data shows the FACS output obtained following the co-culture and SNDX-5613 treatment of primary AML cells. This will be followed by a demonstration of the quantity and quality of RNA extracted from sorted cells. The results of expression profiling carried out by reverse-transcriptase qPCR and bulk RNA sequencing will then be presented. Lastly, flow cytometry results using anti-phospho-STAT5 will be shown for evaluation of the effect of SNDX-5613 on the cell lines MV4-11 and Kasumi-1, primary *UBTF*-TD samples, and when in combination with the FLT3 inhibitor, Gilteritinib, for which the conditions of optimal effect were determined.

3.2 Fluorescence-activated cell sorting (FACS) analysis of AML and MSC cells

To investigate the effect of SNDX-5613 on global gene expression, primary AML cells harboring the *UBTF*-TD alteration were co-cultured with MSCs and treated with 250nM SNDX-5613, or DMSO on days 1, 4, 7, and 10. Appropriate splitting and refreshing of the medium was carried out in between. Cells were harvested for sorting via fluorescence-activated cell sorting (FACS) on days 7 and 12 of treatment with the aim of obtaining pure AML cells. Anti-human CD73-BV421, anti-human CD33-APC, and anti-human CD45-APC were used with an initial gating strategy established on unstained cells. CD73+ cells were discarded, and CD73- cells were sorted further using CD33 and CD45, specifically selecting AML cells (positive cells). A small portion of these sorted cells were tested for sorting quality. 1-4% MSC contamination post-sorting was observed.

***Figure 3.1*- FACS Analysis of Treated Cells Harvested on Day 7 and Day 12**

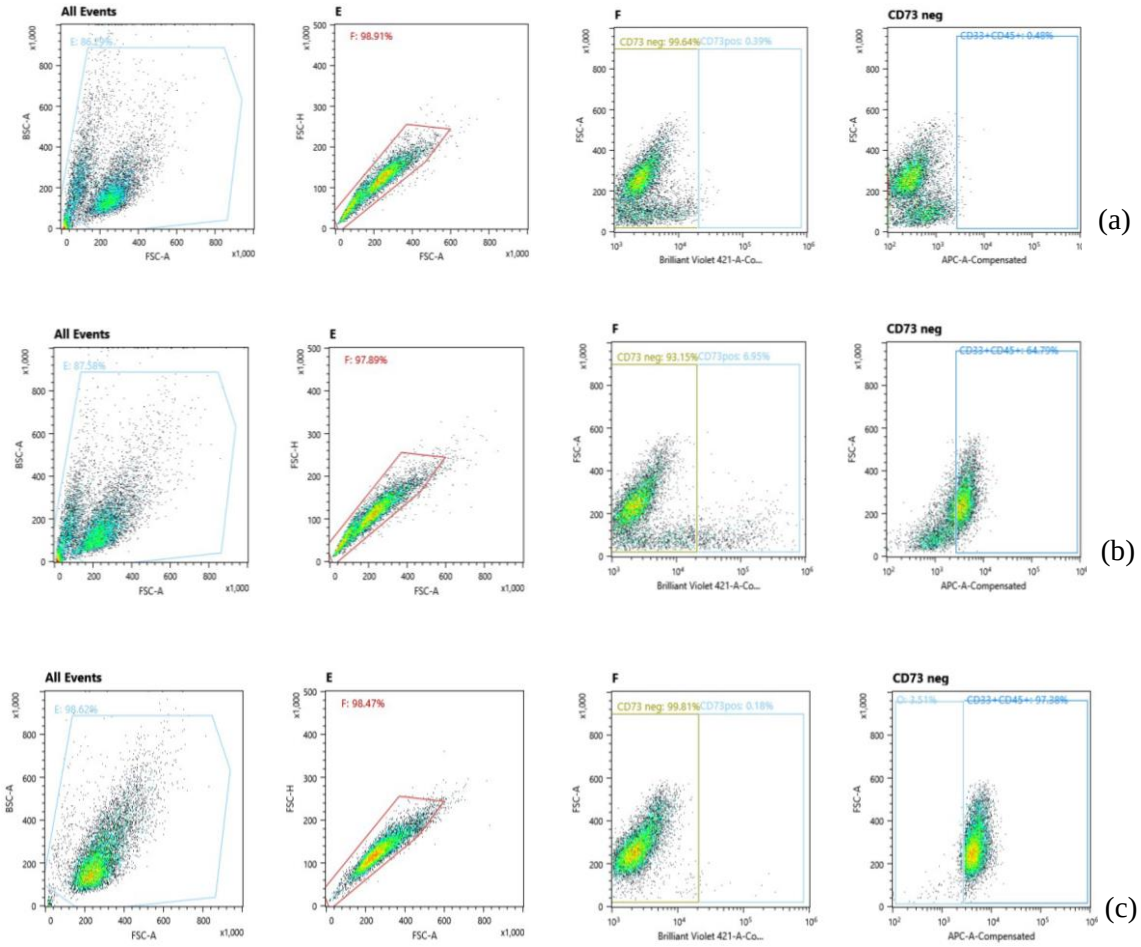

FACS output showing gating of all cells, single cells, and antibody binding expression using anti-human CD73, APC anti-human CD33, and APC anti-human CD45 to obtain a pure AML cell sample separate from MSCs. (A) Unstained cells used to establish a gating strategy. (B) Harvested samples during sorting. (C) Post-sorting quality assurance.

3.3 RNA Quantification by Qubit™

RNA was extracted from mock and treated samples harvested on day 7 and day 12 using Nucleospin® RNA kit (Macherey-Nagel, Düren, Germany). The yield of extracted RNA was analyzed by Qubit™ RNA HS (High Sensitivity) Assay (ThermoFisher Scientific) on Qubit™ 4 Fluorometer RES00046. This ensured that the quantity of RNA was sufficient for further downstream analysis. For bulk RNA sequencing, it was essential to have at least 300ng of RNA per sample and a final total

volume of 10µl. The table below depicts the RNA yield results for each sample. As one may observe, all values were satisfactory.

Table 3.1 **– The results of RNA Quantification by Qubit™**

Sample	Result x10 (ng/ µl)
1	546
2	566
3	450
4	488
5	476
6	598
7	66
8	336
9	276
10	97.6
11	314
12	165

3.4 RNA Quality Check by Agilent RNA 6000 Nano Reagents

To ensure that the extracted RNA was of satisfactory quality for further downstream analysis, it was necessary to carry out a quality check. This was done using the Agilent RNA 6000 Nano Reagents (Agilent Technologies) which works by separating nucleic acid fragments based on size. *Figure 3.2* depicts an illustration of a successful total RNA scan, in which the first peak is the marker, and the two subsequent peaks correspond to 18S and 28S for eukaryotic RNA. RIN (RNA Integrity Number), an objective measure of total RNA quality, was greater than 8.5 for all samples (highly intact RNA). *Figure 3.3* depicts graphically some of the results obtained from the extracted RNA. All results were adequate.

***Figure 3.2*- Model Example of a Successful Sample Run**

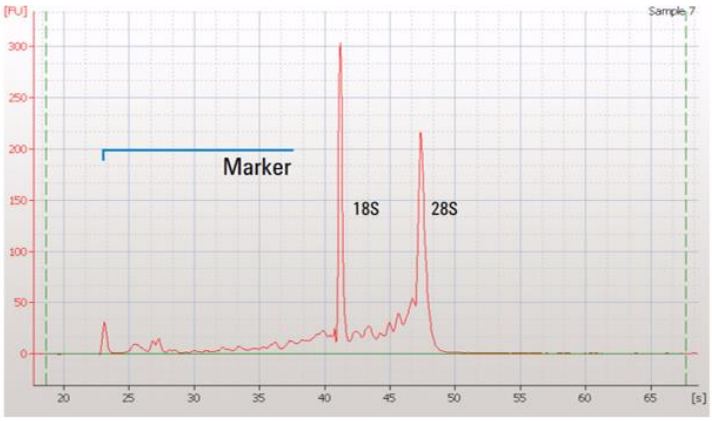

***Figure 3.3*- RNA Quality Check Results using Agilent RNA 6000 Nano Reagents**

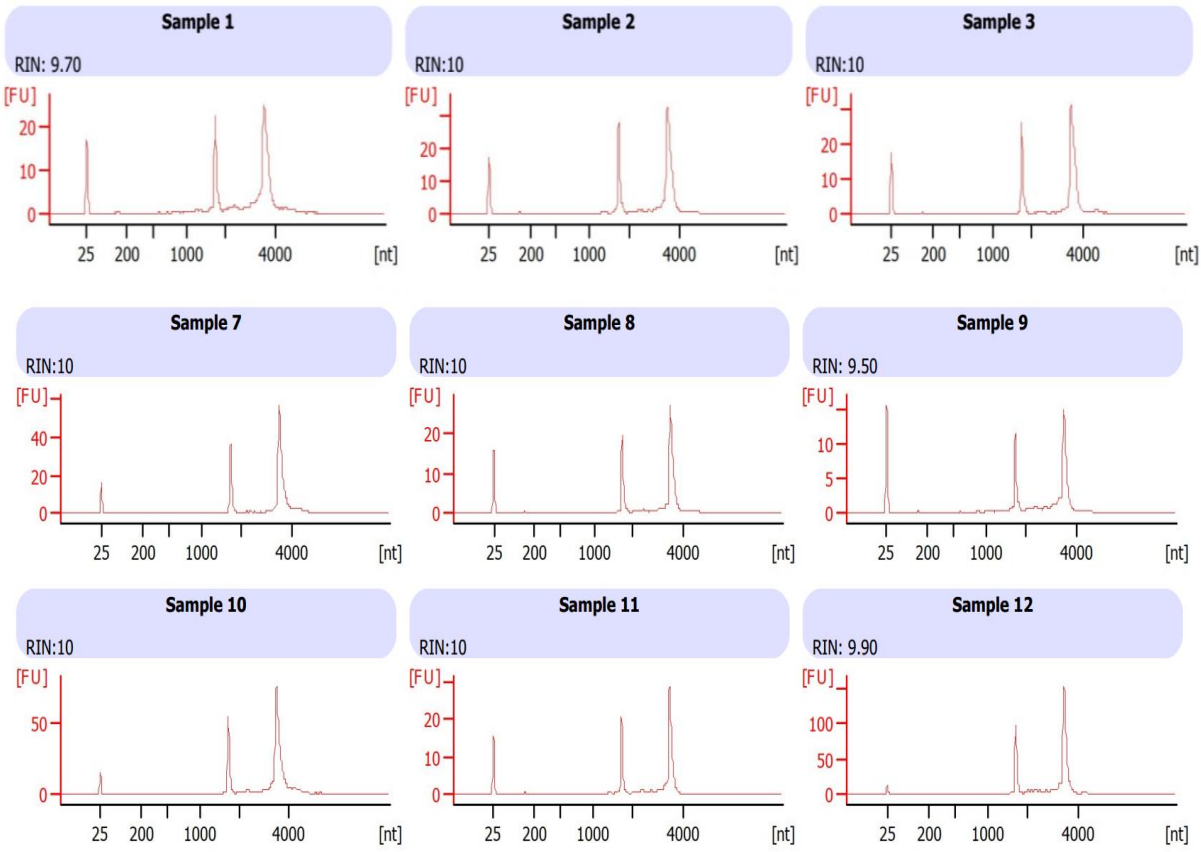

The above graphs represent the results obtained from the RNA quality check. As can be seen, all samples show 1 marker peak and 2 ribosomal peaks and a RIN between 8.5 and 10. This was true for all samples.

3.5 Expression Profiling of Reverse-Transcriptase qPCR

Following cDNA synthesis from extracted RNA, a few genes were chosen for RT-qPCR to analyze the effect of SNDX-5613 on global gene expression prior to RNA sequencing. The chosen genes are downstream targets that depend upon the menin-MLL interaction; therefore, we expected to see downregulation following treatment which would be unobserved in mock samples. During analysis, it was confirmed that there were no primer dimer amplifications and only one PCR product obtained for the target genes and for the TBP internal control. The below figures demonstrate fold change for mock and SNDX-5613 samples harvested on day 7 of treatment.

***Figure 3.4*- RT-qPCR Results for *MEIS1* Day 7**

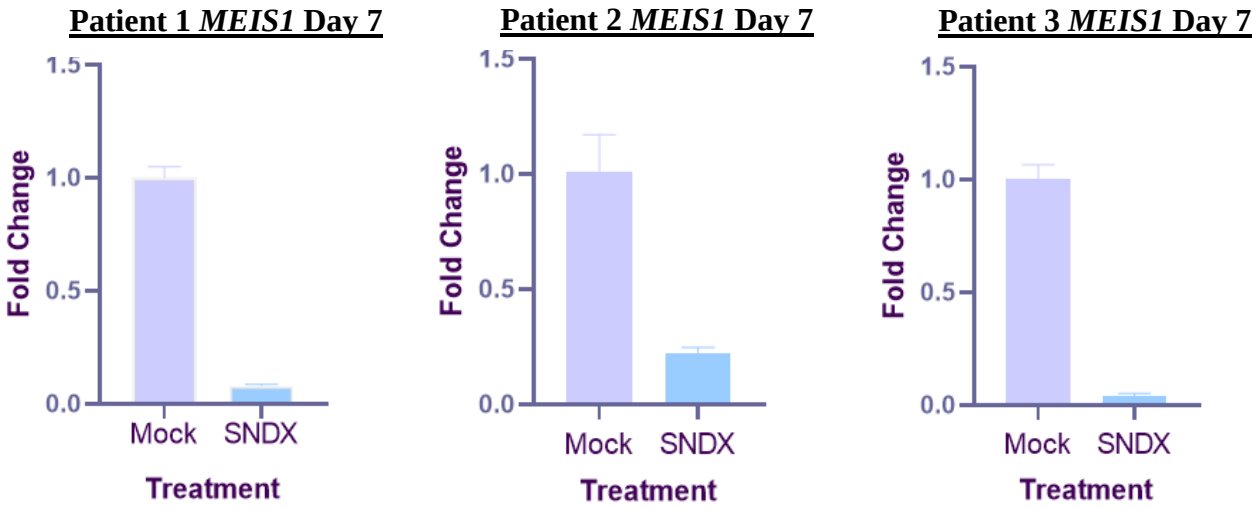

MEIS1 is an essential regulator for leukemia stem cell (LSC) maintenance and it's enforced expression could induce the transformation of a normal hematopoietic system to leukemia. The above graphs show >50% downregulation of this gene following treatment with SNDX-5613 (250 nM), as expected.

***Figure 3.5*- RT-qPCR Results for *FLT3* Day 7**

Patient 1 *FLT3* Day 7

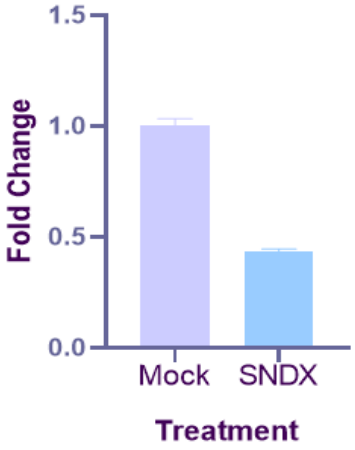

Patient 2 *FLT3* Day 7

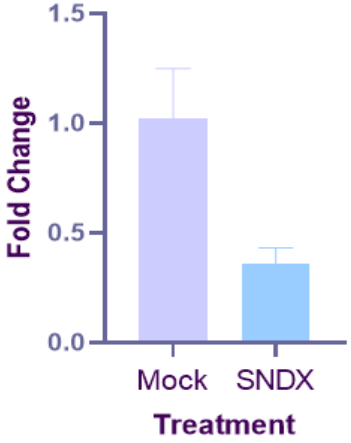

Patient 3 *FLT3* Day 7

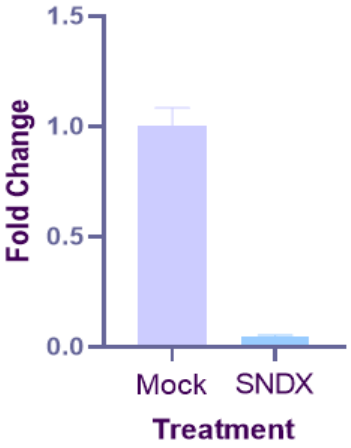

FLT3 is a putative transcriptional *MEIS1* target and is one of the genes most dramatically downregulated following Menin-MLL inhibition in *NPMI*^{mut} AML. The above graphs show >50% downregulation of this gene following treatment with SNDX-5613 (250 nM), as expected.

***Figure 3.6*- RT-qPCR Results for *PBX3* Day 7**

Patient 1 *PBX3* Day 7

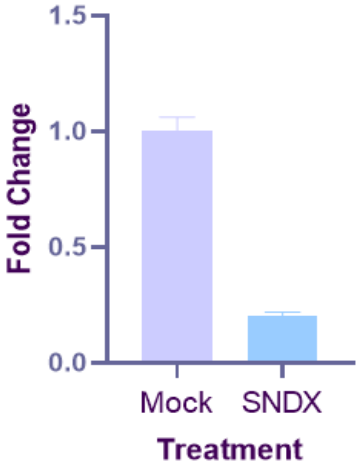

Patient 2 *PBX3* Day 7

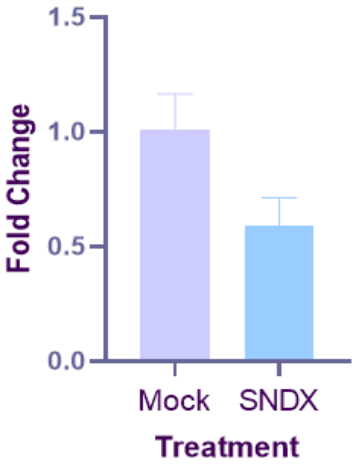

Patient 3 *PBX3* Day 7

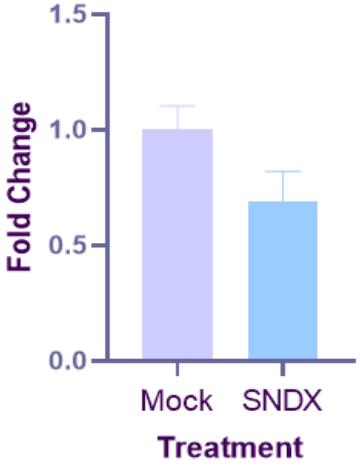

PBX3 is highly expressed in LSCs, maintains LSC capacity, and inhibits LSC apoptosis. The above graphs show expected downregulation of this gene following treatment with SNDX-5613 (250 nM).

***Figure 3.7*- RT-qPCR Results for *MEF2C* Day 7**

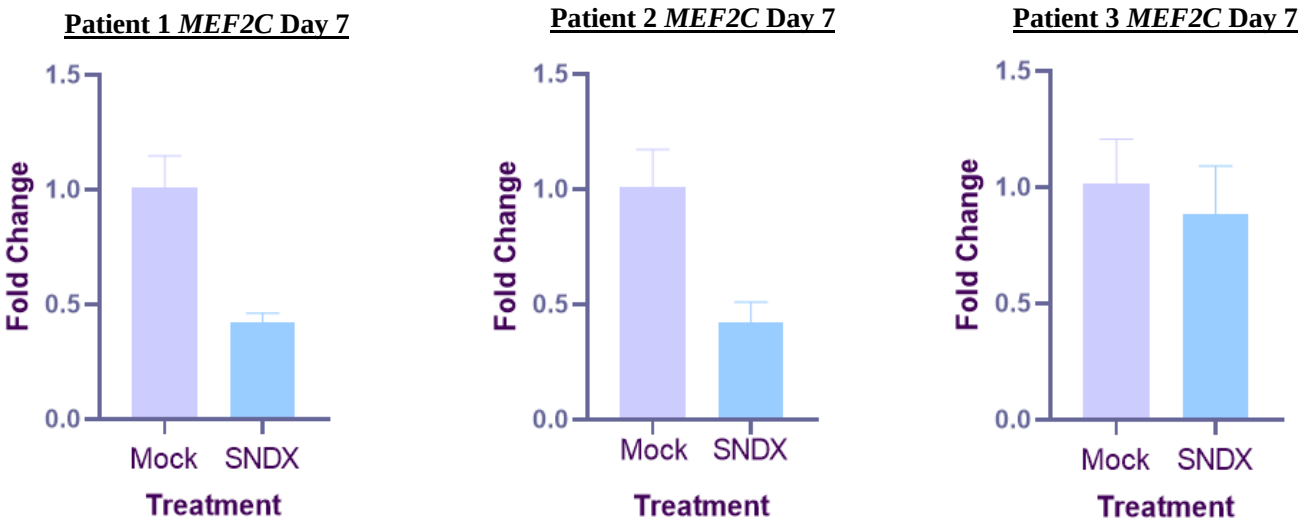

Myocyte enhancer factor 2C *(MEF2C*) is recognized as a cooperating oncogene in AML. The above graphs show downregulation of this gene following treatment with SNDX-5613 (250 nM), especially in patient 1 and patient 2 in which >50% downregulation is observed.

***Figure 3.8*- RT-qPCR Results for *HOXA9* Day 7**

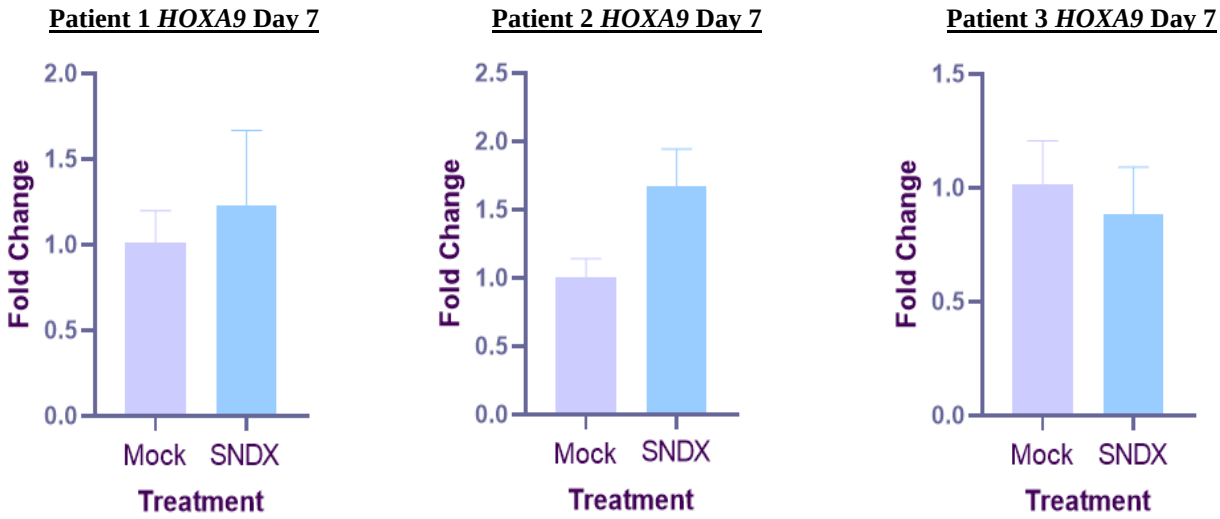

HOXA9 dysregulation is needed and sufficient for leukemic transformation. It functions as a pioneer transcription factor and assembles leukemia-specific enhancers via recruitment of the MLL3/MLL4 complex to control gene expression and the development of leukemia. Interestingly, the above graphs show upregulation of this gene in 2 samples following treatment with SNDX-5613 (250 nM).

***Figure 3.9*- RT-qPCR Results for *CD11b* Day 7**

Patient 1 *CD11b* Day 7

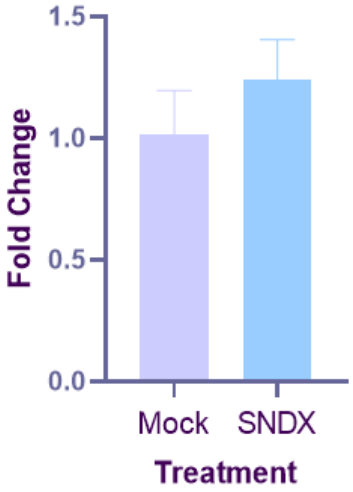

Patient 2 *CD11b* Day 7

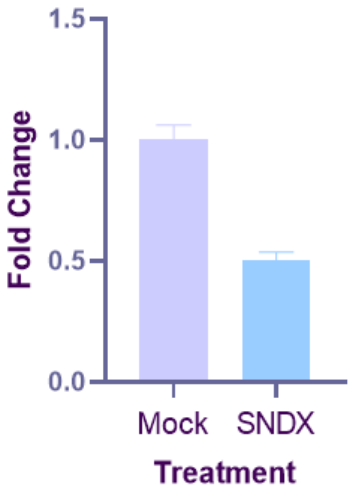

Patient 3 *CD11b* Day 7

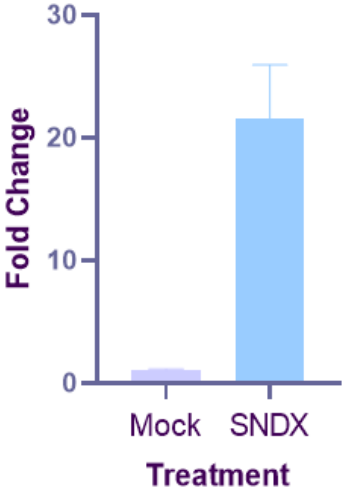

CD11b is as a differentiation marker for cells belonging to the myeloid-monocytic lineage. Therefore, we would expect to see upregulation of this gene following treatment with SNDX-5613 (250 nM). Upregulation of this gene can be observed in the results of patient 1 and patient 3.

***Figure 3.10*- RT-qPCR Results for *MNDA* Day 7**

Patient 1 *MNDA* Day 7

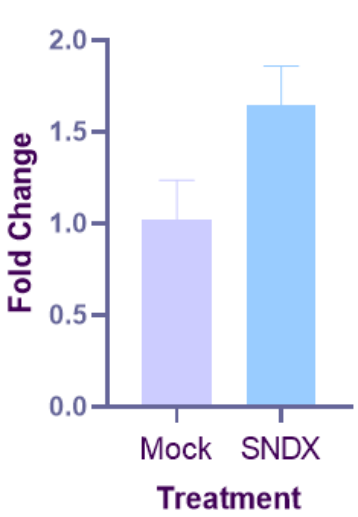

Patient 2 *MNDA* Day 7

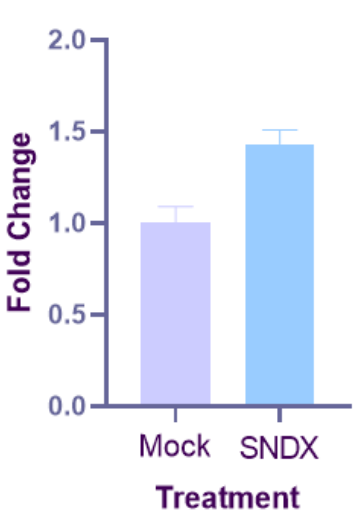

Patient 3 *MNDA* Day 7

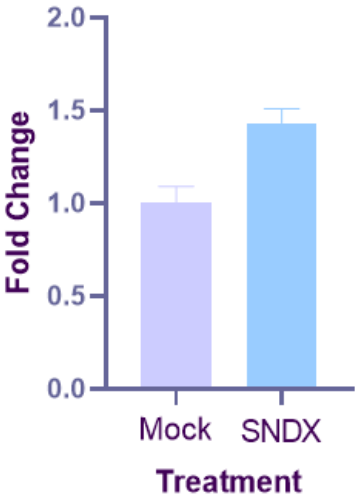

MNDA is being used as a differentiation marker due to its association with myeloid and monocytic differentiation in acute leukemia. Thus, we would expect to see an upregulation of this gene follow treatment with SNDX-5613 (250nM). The above graphs show upregulation of *MNDA* in all 3 patient samples.

3.6 Expression Profiling of Bulk RNA-Sequencing

The previously established transcriptional similarities between *UBTF*-TD AMLs and other better-defined AML subtypes such as *MLL*-r AML, *NUP98*r AML, and *NPM1* AML have led to the hypothesis that all of these AML subtypes may follow similar oncogenic programs. Therefore, when analyzing RNA-sequencing data, focus was placed on the target genes of the forementioned AML subtypes' oncoproteins. The volcano plots and heatmaps below show that many of these expected genes were in fact downregulated following treatment with SNDX-5613.

***Figure 3.11*- RNA-Sequencing Day 7 Volcano Plot**

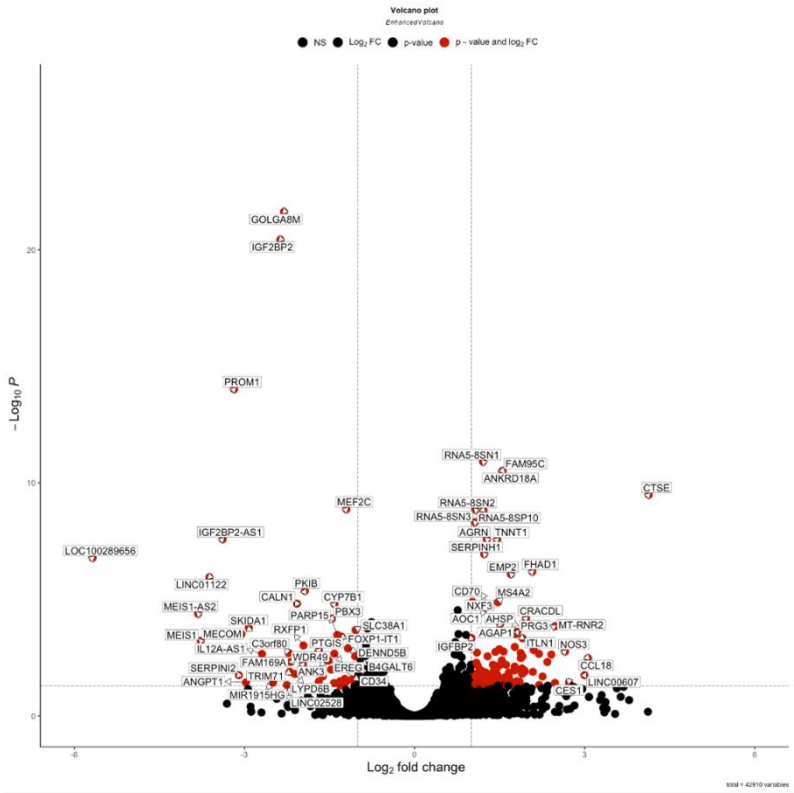

This volcano plot demonstrates 142 up-regulated genes and 58 significantly down-regulated genes following treatmemt. Amongst the downregulated genes one may easily point out *MEF2C*, *IGF2BP2*, *PBX3* and *MEIS1* which are all well-known targets of MLL and NUP98 oncoproteins.

***Figure 3.12*- RNA-Sequencing Day 7 Heatmap**

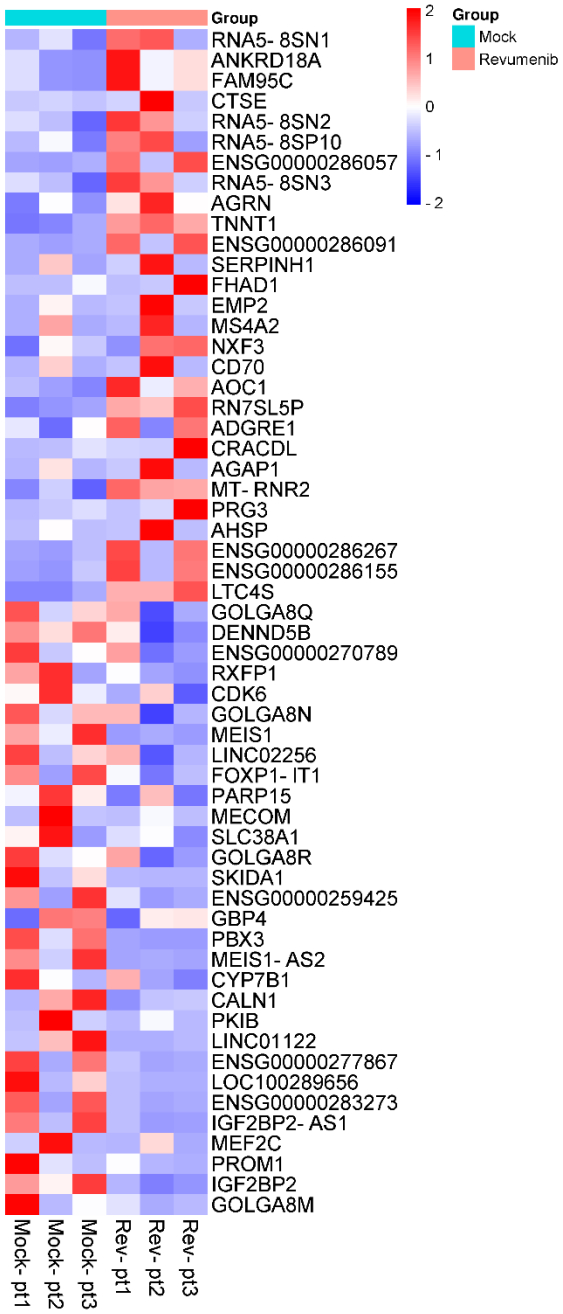

This heatmap shows the top 40 genes up-regulated and down-regulated in *UBTF*-TD AML samples upon menin inhibition on day 7. By looking at the genes significantly changed in a downregulated manner, we can once again see the genes of interest: *MEIS1, PBX3, MEF2C, PROM1 and IGF2BP2*

***Figure 3.13*- RNA-Sequencing Day 12 Volcano Plot**

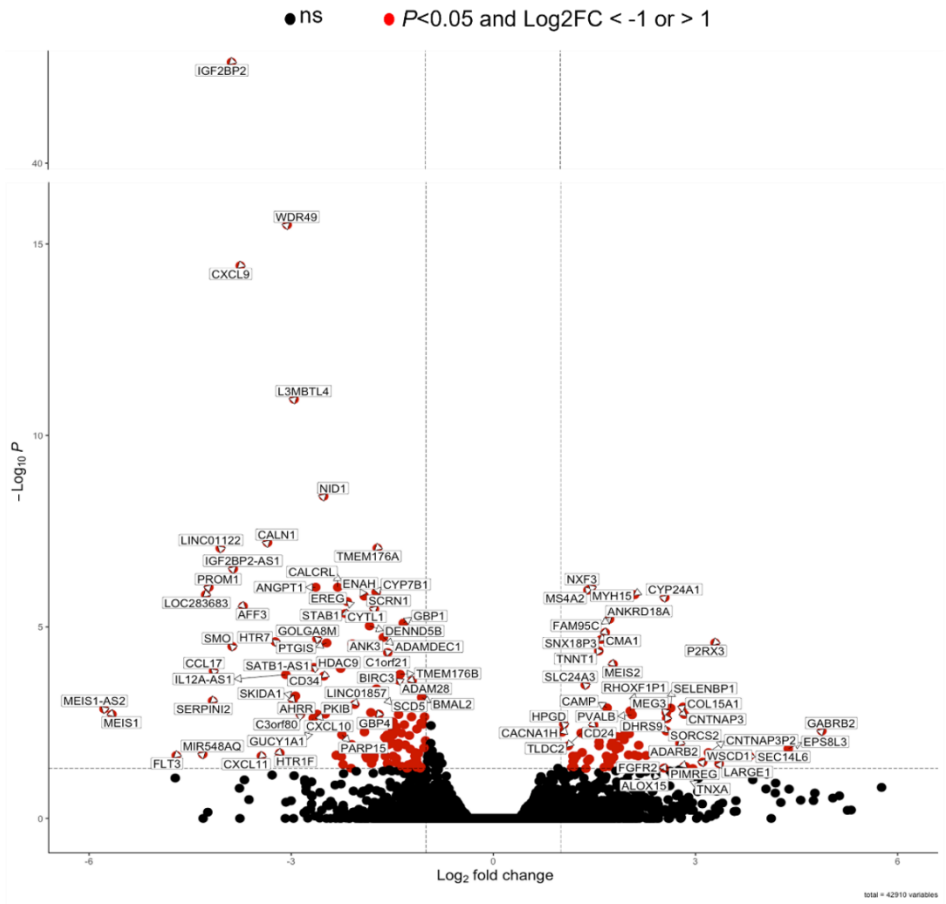

This volcano plot demonstrates 93 up-regulated genes and 237 significantly down-regulated genes following treatment with SNDX-5613 (250nM). *IGF2BP2*, *PROM1*, *MEIS1*, and *FLT3* are seen amongst the downregulated genes, which are all MLL-r, NPM1, and NUP98 oncoprotein target genes.

***Figure 3.14*- RNA-Sequencing Day 12 Heatmap**

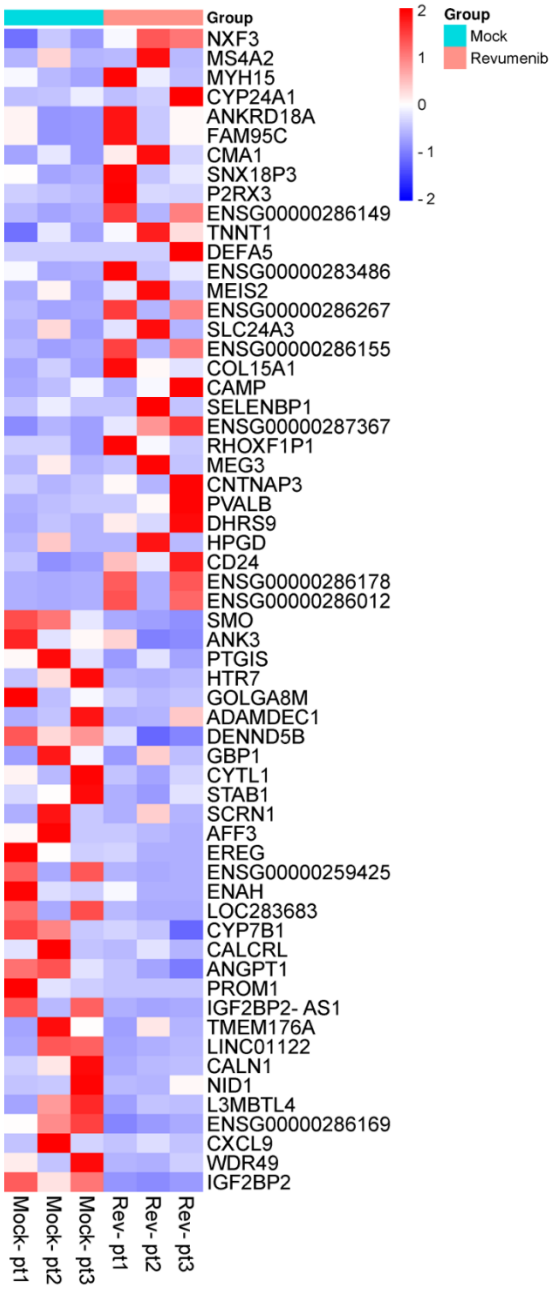

This heatmap shows the top 40 genes up-regulated and down-regulated in *UBTF*-TD AML samples upon menin inhibition on day 12. Here again we see genes of interest being downregulated: *PROM1* and *IGF2BP2*.

Gene Set Enrichment Analysis (GSEA) was carried out on the collected RNA-sequencing data to group the genes of interest by biological pathway and understand the effect of SNDX-5613 on such pathways and their associated functions. The figures below demonstrate the main findings obtained.

***Figure 3.15*- GSEA Looking at NUP98 Fusion Target Genes**

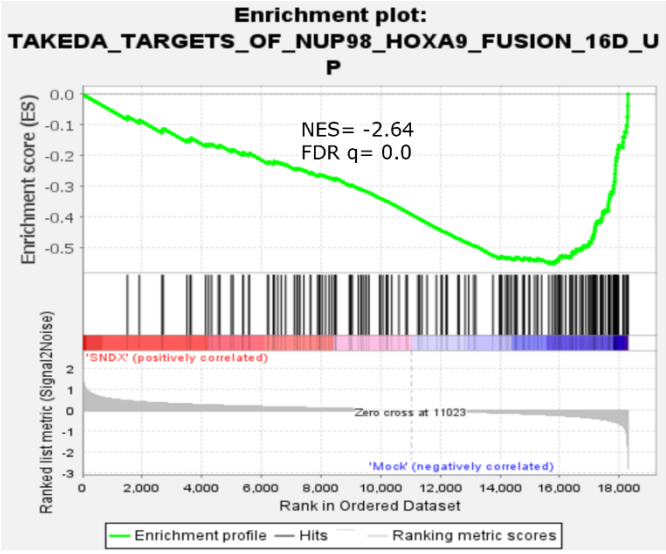

GSEA showing a set of NUP98 fusion target genes that are enriched in the mock group, indicating that SNDX perturbs the leukemic stem cell program.

***Figure 3.16*- GSEA Looking at Hematopoietic Stem Cell Related Genes**

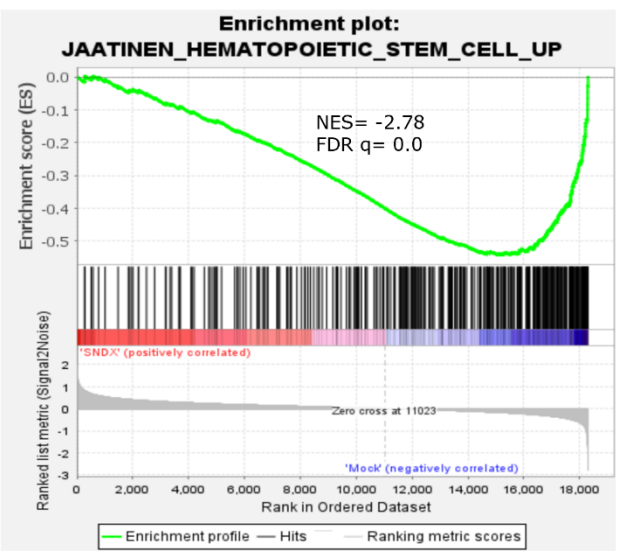

GSEA showing suppression of haematopoietic stem cell related genes upon treatment.

3.7 Phospho-STAT5 Analysis Following SNDX-5613 Treatment

UBTF-TD AML is often accompanied by mutations in FMS-like tyrosine kinase 3 (*FLT3*), specifically *FLT3*-ITD, resulting in constant activation of the FLT3 signal which gives a proliferation advantage to leukemic cells and subsequent collaboration in transformation. Since inhibition of the menin-MLL interaction targets *FLT3* transcriptionally, we set out to investigate the effect of SNDX-5613 on FLT3 in *UBTF*-TD patient samples. As we observed suppression of FLT3 expression by Menin inhibition at genomic level, we sought to analyze the downstream pathway of FLT3 looking at phopho-STAT5 following treatment. We hypothesized a downregulation of phospho-STAT5 following treatment which could be observed by flow cytometry.

The initial experiment was carried out on the MV4-11 cell line; these cells harbor an *MLL*-r alteration which should be targeted by SNDX-5613. Therefore, the same hypothesis applies. Cells were treated on day 0 with 25nM SNDX-5613, then harvested, stained, and analyzed on day 4 using PE anti-STAT5 Phospho Antibody.

***Figure 3.17*- Phospho-STAT5 Analysis on MV4-11 Cell Line**

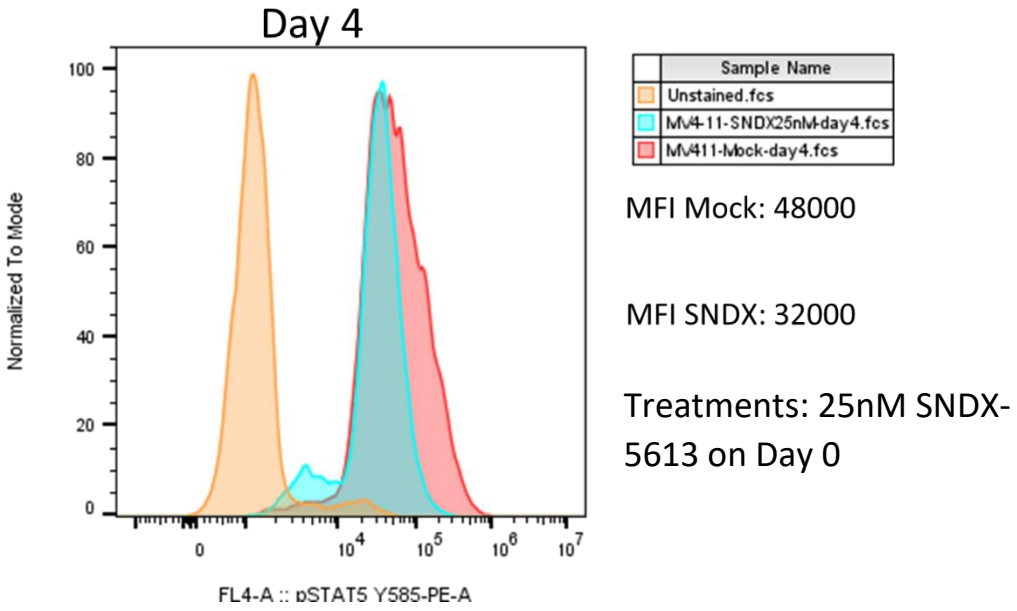

A left shift observed by the blue peak indicates a downregulation of phospho-STAT5 and thus FLT3 following treatment with SNDX-5613 (25nM).

Following these promising results, the experiment was repeated on primary *UBTF*-TD patient samples. *UBTF*-TD samples were co-cultured and treated with 250nM SNDX on day 0 and day 4 with no further treatments in between. Cells were harvested, stained, and analyzed on day 8 and day 11. On day 4, cells were cultured in cytokine-free SFEM to avoid re-activation of the SNDX-5613-deactivated phospho-STAT5 by IL-3 and FLT3-ligand.

***Figure 3.18*- Phospho-STAT5 Analysis on *UBTF*-TD Primary Samples**

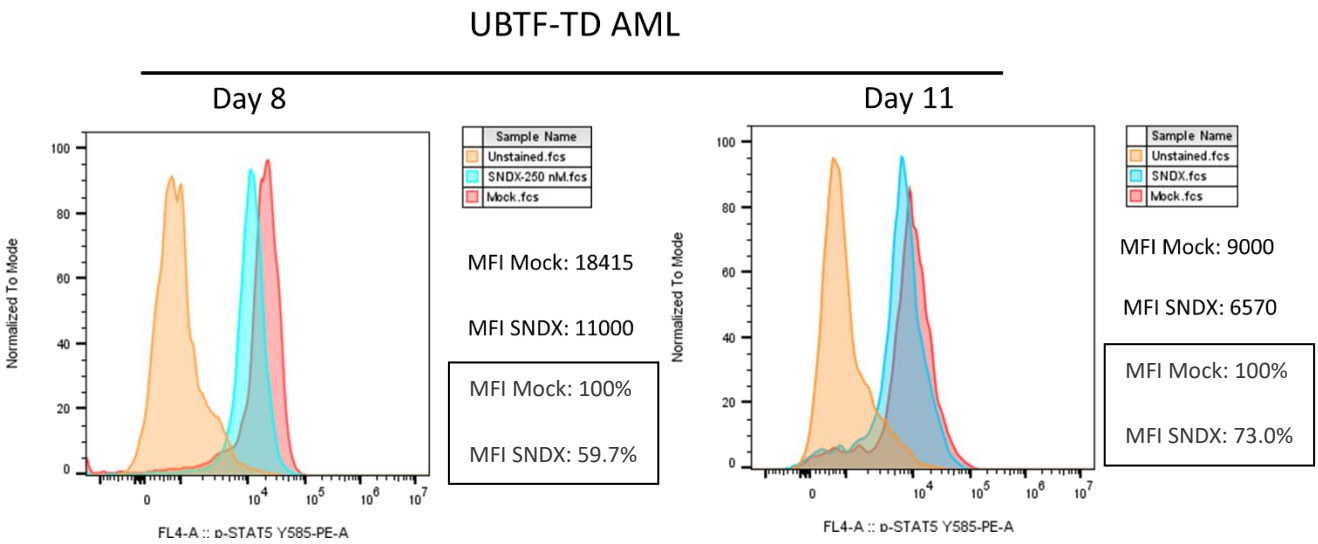

Treatments: 250 nM SNDX-5613 on days 0 and 4

Here again, a left shift was observed by the blue peak on both days indicating downregulation of phospho-STAT5. This is reduced on day 11, indicating a potential reduction in efficacy of SNDX by time.

3.8 Investigating the Combination of SNDX-5613 and Gilteritinib Therapy

Previous studies on *NUP98*-r and *MLL*-r AMLs have shown that when a Menin inhibitor is combined with an FLT3 inhibitor, a synergistic effect may be observed, leading to a reduction in leukemia cell proliferation and leukemic gene expression. As a result, we set out to investigate the effect of combination treatment on *UBTF*-TD AML samples using SNDX-5613 (250nM) and the FLT3

inhibitor, Gilteritinib; a synergistic effect between pathways is hypothesized. Once again, results were analyzed by looking at changes in phospho-STAT5 expression via flow cytometry.

Investigations were initiated on the cell lines Kasumi-1 and MV4-11. Since Kasumi-1 cells have the RUNX1::ETO fusion, we did not expect SNDX-5613 and Gilteritinib to target this alteration individually or synergistically, making these cells the negative control. For this experiment, two Gilteritinib concentrations were chosen based on Gilteritinib's IC50: 1nM and 10nM.

***Figure 3.19*- Phospho-STAT5 Analysis of Combination Therapy on Kasumi-1 Cells**

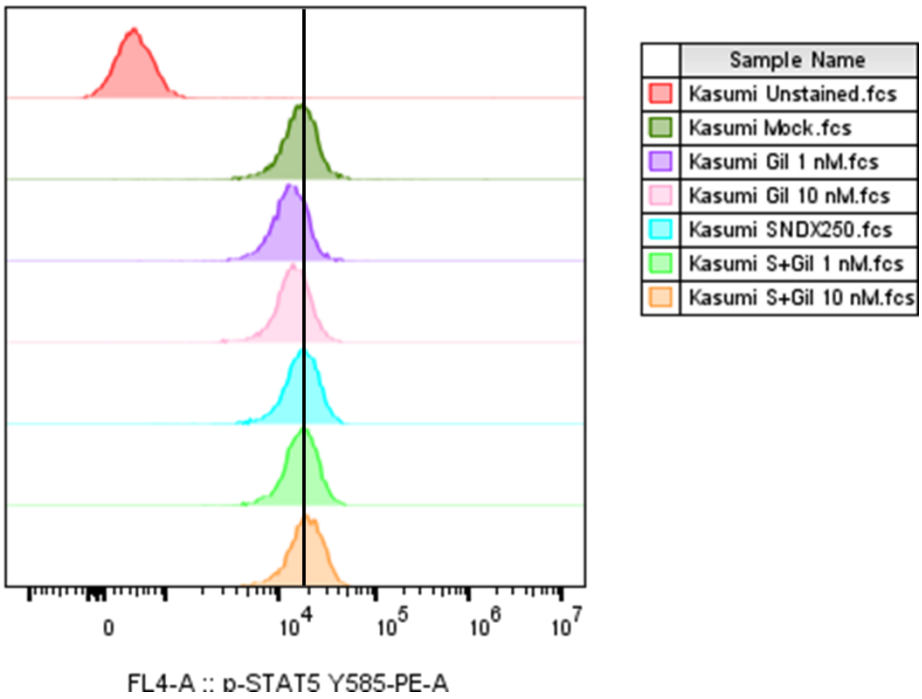

As can be seen, all peaks resemble the result for mock meaning that there were no changes seen when Kasumi-1 cells were treated with SNDX-5613, Gilteritinib, or their combination in varying concentrations, as expected.

***Figure 3.20*- Phospho-STAT5 Analysis of Combination Therapy on MV4-11 Cells**

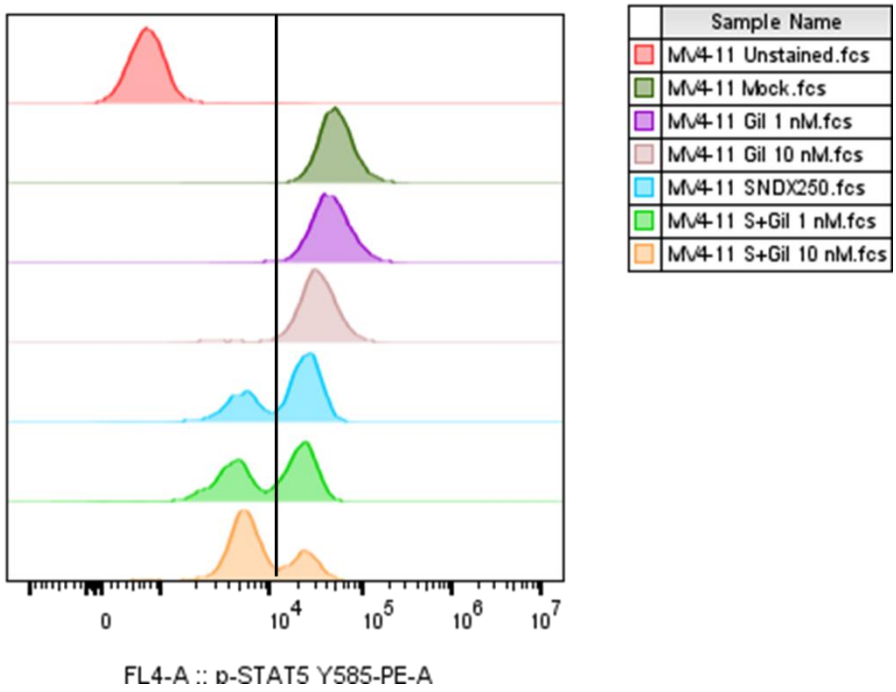

Following treatment of MV4-11 cells, various left shifts were observed, indicating that phospho-STAT5 and FLT3 were being downregulated following treatment. The most notable change was that of the combination of SNDX-5613 (250nM) with 10nM Gilteritinib.

The above results complimented the hypothesis that SNDX-5613 and Gilteritinib could work synergistically in *UBTF*-TD samples. Therefore, we sought to investigate this in primary samples. Although Gilteritinib has been previously used in literature and its IC50 in cell lines has been widely acknowledged, there is a lack of information on its use in primary samples. Therefore, there was a need to discover the time point and concentration of optimal drug activity in order to have a fair assessment of the effect of combination therapy.

To do this, primary samples were treated with 3 concentrations of Gilteritinib: 10nM, 100nM, and 1000nM, and cells were harvested at two time points following treatment: 30 minutes, and 2 hours. Phospho-STAT5 was then analyzed via flow cytometry.

***Figure 3.21*- Gilteritinib Time and Concentration Series**

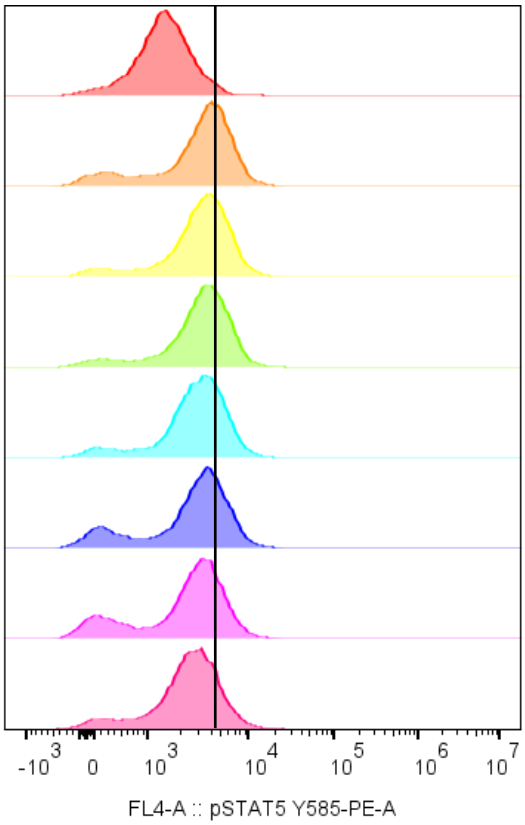

	Sample Name	Subset Name
	Unstained.fcs	pSTAT5 Y585-PE-A subset
	Mock.fcs	pSTAT5 Y585-PE-A subset
	30min-10nM.fcs	pSTAT5 Y585-PE-A subset
	30min-100nM.fcs	pSTAT5 Y585-PE-A subset
	30min-1000nM.fcs	pSTAT5 Y585-PE-A subset
	2hr-10nM.fcs	pSTAT5 Y585-PE-A subset
	2hr-100nM.fcs	pSTAT5 Y585-PE-A subset
	2hr-1000nM.fcs	pSTAT5 Y585-PE-A subset

MFI Unstained	41.5%
MFI Mock	100%
MFI 30 mins, 10nM	96.7%
MFI 30 mins, 100nM	97.2%
MFI 30 mins, 1000nM	86.4%
MFI 2 hrs, 10nM	87.0%
MFI 2 hrs, 100nM	78.6%
MFI 2 hrs, 1000nM	74.1%

Phospho-STAT5 analysis revealed a left shift in all peaks, most noteworthy at higher time points and concentrations. Phospho-STAT5 and FLT3 were most effectively downregulated at 2 hours and when treated with 1000nM Gilteritinib.

Despite the previous results, 100nM Gilteritinib was chosen for testing the combination treatment in primary *UBTF*-TD samples. This is because 1000nM is too high for future *in vivo* application. Cells were co-cultured for 7 days and treated with 250nM SNDX-5613 or DMSO (mock) on days 1, 5, and 7. On day 7, SNDX-5613/DMSO treatment was also followed by 100nM Gilteritinib, and cells were harvested, stained with anti-phosphoSTAT5, and analyzed after 2 hours.

***Figure 3.22*- Phospho-STAT5 Analysis of Combination Treatment on *UBTF*-TD Samples**

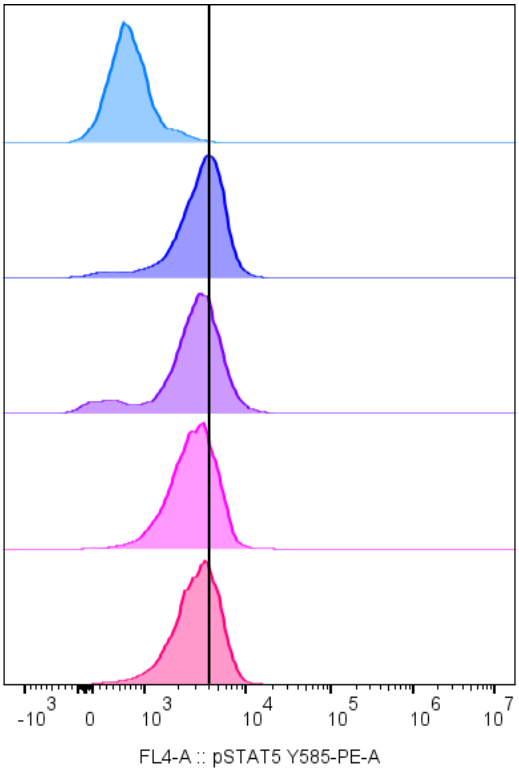

	Sample Name	Subset Name
	Unstained	pSTAT5 Y585-PE-A subset
	Mock	pSTAT5 Y585-PE-A subset
	Gilteritinib-100nM	pSTAT5 Y585-PE-A subset
	SNDX-250nM	pSTAT5 Y585-PE-A subset
	SNDX+Gilteritinib.fcs	pSTAT5 Y585-PE-A subset

MFI Unstained	18.9%
MFI Mock	100%
MFI Gilteritinib-100nM	86.8%
MFI SNDX-250nM	81.6%
MFI Combination	90.0%

The above results display that although there is a left shift and thus pSTAT5/FLT3 downregulation when primary cells are treated with SNDX-5613 (250nM) and Gilteritinib (100nM) individually, a synergistic effect is not observed when the two are applied in combination.

Chapter 4 – Discussion and Conclusion

In this study, we have looked at AMLs with a recently discovered recurrent alteration in pediatric patients called upstream binding transcription factor tandem duplications (*UBTF*-TDs) and its response to the Menin-MLL inhibitor SNDX-5613. In line with unpublished data, indicating that UBTF-TD localizes at the proximity of Menin and MLL1, we showed that this lesion-defining AML subtype is reliant on the Menin-MLL protein-protein interaction. When the Menin-MLL interaction is disturbed by the inhibitor, results have shown changes that correspond directly to leukemia suppression and induction of differentiation. This was depicted specifically by the reduction in the expression of key genes that play a role in leukemogenesis, upregulation of genes that promote cell differentiation, and a depletion of cell stemness presented by GSEA. Importantly, we have shown that the transcriptional program of *UBTF*-TD AMLs overlaps significantly with other AML subtypes that were previously shown to co-cluster with it transcriptionally. This means that we can apply further successful research advances achieved on these AML subtypes and expect promising results for *UBTF*-TD AML patients.

This project has contributed to the understanding that Menin inhibitors are able to offer therapeutic value to AML subtypes that are dependent upon the Menin-MLL interaction and displays *HOXA/HOXB* overexpression. We have already seen this to be true for *MLL*-r AML, *NUP98::NSD1* AML, and *NPM1*-mutated AML. Future studies may determine the therapeutic efficacy of the Menin inhibitors to be applicable for *DEK::NUP214* AML and *MN1*-mutated AML, amongst others, which follow similar transcriptional programs and co-cluster with *MLL*-r AMLs but have yet to be investigated (Issa, Ravandi et al. 2021, Rasouli, Blair et al. 2023, Issa, Aldoss et al. 2022).

Here, we have shown the impact of SNDX-5613 on patient-derived *UBTF*-TD AML samples. Often lacking in therapy-related studies is the use of primary cell samples harboring the alteration of interest; genetically engineered immortal cell lines are typically the chosen route. Cell lines are made to resemble the primary cells closely in all aspects, and advantageously they are cheaper, abundant in supply, easy to work with, and ethically sound. However, they fail to display the heterogeneity of

AML which could potentially have a significant impact on treatment response. Therefore, the behavior of cell lines to drug treatments might be inaccurate and unreliable (Kaur, Dufour 2012).

For some experiments in this project, MV4-11 cell lines were used, which have an *MLL*-r alteration, and exhibit elevated *HOXA/MEIS1* gene expression. Most experiments were tested or retested on patient-derived AML samples and are thus accurate to the experimental aim. Going forward, it would be useful to establish *UBTF*-TD cell lines that can be used in conjunction with primary samples, for freer testing and for the limited primary material to be used only following favorable results on cell lines.

SNDX-5613 binds to chromatin-bound Menin and results in the global loss of this protein from chromatin. This in turn selectively separates both MLL1 and UBTF-TD from each other and chromatin at the loci of specific genes that have important roles in leukemogenesis and leukemia maintenance. As a result, pathological aberrant gene expression is halted (Fiskus, Mill et al. 2023). Interestingly, we have seen the substantial downregulation of *MEIS1* and *FLT3* upon treatment, a finding that is well in line with many other projects that have looked at Menin-MLL inhibitors in different AML subtypes (Rasouli, Blair et al. 2023, Issa, Aldoss et al. 2022). *MEIS1* is expressed in haematopoietic stem cells, and expression is downregulated with differentiation. On a genetic level, the transcription of *FLT3* is dependent on cooperating events between *MEIS1* and *HOXA9* and overexpression of these two genes may be sufficient to drive leukemogenesis (Blasi, Bruckmann 2021). Similarly, the interaction of *HOXA9, MEIS1,* and *PBX3* is accountable for haematopoietic transformation in *MLL*-r leukemia (Guo, H., Chu et al. 2017). Therefore, it is interesting to note that while *MEIS1*, *FLT3* and *PBX3* were successfully targeted by SNDX-5613 in *UBTF*-TD cells, *HOXA9* did not appear to have notable downregulated changes. This suggests that downregulation of *HOXA9* is not necessary for leukemia suppression, an observation previously made in *NUP98*-r AML (Rasouli, Blair et al. 2023). Importantly, *FLT3* was seen to be downregulated on day 12, a result of its secondary genetic nature as a putative transcriptional *MEIS1* target (Dzama, Steiner et al. 2020). This showed that SNDX-5613 can target both primary (*MEIS1*) and secondary (*FLT3*) genetic events. Moreover, such results demonstrate that SNDX-5613 can be effective in the presence of concomitant

somatic mutations like *FLT3*-ITD and *WT1*. This should be supported in future studies by cell proliferation and apoptotic analysis.

FLT3-ITD is a common somatic mutation found in *UBTF*-TD AMLs; it itself is a leukemic driver and thus, an important therapeutic target (Daver, Schlenk et al. 2019). FLT3 inhibitors have seen some success in cell-cycle arrest, reducing cell proliferation, and inducing apoptosis, but on a clinical level, single treatment is not up to par (Dzama, Steiner et al. 2020). In this study, we explored the effects of the FLT3 inhibitor Gilteritinib in combination with SNDX-5613, hypothesizing synergism. When in combination, we observed that the response to treatment wasn't improved when compared to single treatments, and in fact, SNDX-5613 individual treatment had a more favorable effect. This is a surprising result when compared to previous findings found in the literature, but then again, such studies were carried out on cell lines and did not target *UBTF*-TD specifically. Moreover, in this case we looked at phospho-STAT5 signaling to measure *FLT3* activation indirectly, and perhaps by investigating if other signaling pathways, such as the ERK/MPK, P13K pathway, or directly analyzing *FLT3* activation after treatment, different results might be obtained.

Following the satisfactory results of SNDX-5613 monotreatment on *UBTF*-TD cells, it was important to begin focusing on combination treatment. In the recent phase 1 first-in-human clinical trial which tested SNDX-5613 on patients with *MLL*-r or mutated *NPM1* AML, acquired somatic mutations in *MEN1* were identified, leading to therapy resistance (Perner, Stein et al. 2023). Such mutations were found at the inhibitor-Menin interface, hindering Menin's release from chromatin but leaving the menin-MLL1 interaction intact. Specifically, this drug resistance is seen as a result of recurrent changes in the amino acid residues M327, G331, T349, and S160 (Perner, Stein et al. 2023). The proposed strategy here is for second generation inhibitors to still disturb the Menin-MLL interaction, but simultaneously avoid the residues that have been affected by acquired mutations. Importantly, the development of this resistance validates that the Menin-MLL interaction is the key to leukemic onset and progression (Perner, Stein et al. 2023). Such studies have provided *UBTF*-TD researchers with the advantage of knowledge; the most important aspect of drug resistance is anticipation and prediction.

Continuation of combination therapy investigations is a must; drugs with non-overlapping profiles of resistance-conferring mutations can bypass resistance by exerting a synergistic potent effect to ensure that resistant sub-clones do not survive or escape, and through the unlikeliness that multiple genetic changes would occur to induce resistance (Fiskus, Mill et al. 2023, Pisa, Kapoor 2020). For example, in this project we have explored the combination of SNDX-5613 with Gilteritinib, a current standard of care (SOC) treatment, but another idea would be to test the combination of SNDX-5613 with Shikonin, a WT1 inhibitor (Guo, Z., Sun et al. 2022). Moreover, SNDX-5613 is currently undergoing phase II trials to test its combination with chemotherapy, specifically fludarabine and cytarabine (Children's Oncology Group 2023). It's useful to keep in mind that bypassing resistance can occur in many ways, if needed. We have seen that Menin has multiple binding sites to MLL1; perhaps the inhibitor could be designed to bind to more than one site since multiple mutations are less likely to occur. Computational modelling and computation drug design should also be used to aid in optimal drug combination development and resistance prediction (Pisa, Kapoor 2020).

In conclusion, we have shown that SNDX-5613 is a viable treatment option for *UBTF*-TD AML, a recurrent AML alteration that is associated with a dismal outcome, poor prognosis, and minimal residual disease (MRD) positivity. This study may serve as a prelude for further studies needed to approve *UBTF*-TD patient participation in SNDX-5613 clinical studies. Such studies could include the induction of *UBTF*-TD AML in patient derived xenografts (PDX) to wholly explore the response to SNDX-5613 and treatment combinations in a more reliable and representative model. Results could be further supported by the successful engraftment of a SNDX-5613 resistant clone for combination testing.

References

BLASI, F. and BRUCKMANN, C., 2021. MEIS1 in Hematopoiesis and Cancer. How MEIS1-PBX Interaction Can Be Used in Therapy. *Journal of developmental biology,* **9**(4), pp. 44.

BRENNER, A.K., NEPSTAD, I. and BRUSERUD, Ø, 2017. Mesenchymal Stem Cells Support Survival and Proliferation of Primary Human Acute Myeloid Leukemia Cells through Heterogeneous Molecular Mechanisms. *Frontiers in Immunology,* **8**, pp. 106.

CHILDREN'S ONCOLOGY GROUP, June 25, 2023-last update, A Study of Revumenib in Combination With Chemotherapy for Patients Diagnosed With Relapsed or Refractory Leukemia. Available: https://classic.clinicaltrials.gov/ct2/show/NCT05761171.

CHOUDHARY, C., BRANDTS, C., SCHWABLE, J., TICKENBROCK, L., SARGIN, B., UEKER, A., BÖHMER, F., BERDEL, W.E., MÜLLER-TIDOW, C. and SERVE, H., 2007. Activation mechanisms of STAT5 by oncogenic Flt3-ITD. *Blood,* **110**(1), pp. 370-374.

CIERPICKI, T. and GREMBECKA, J., 2014. Challenges and opportunities in targeting the menin–MLL interaction. *Future medicinal chemistry,* **6**(4), pp. 447-462.

DAVER, N., SCHLENK, R.F., RUSSELL, N.H. and LEVIS, M.J., 2019. Targeting FLT3 mutations in AML: review of current knowledge and evidence. *Leukemia,* **33**(2), pp. 299-312.

DE ROOIJ -, J., ZWAAN, C.M. and VAN DEN HEUVEL - EIBRINK, M., 2015. Pediatric AML: from biology to clinical management. *Journal of Clinical Medicine,* **4**(1), pp. 127-149.

DUPLOYEZ, N., VASSEUR, L., KIM, R., LARGEAUD, L., PASSET, M., L'HARIDON, A., LEMAIRE, P., FENWARTH, L., GEFFROY, S., HELEVAUT, N., CELLI-LEBRAS, K., ADÈS, L., LEBON, D., BERTHON, C., MARCEAU-RENAUT, A., CHEOK, M., LAMBERT, J., RÉCHER, C., RAFFOUX, E., MICOL, J., PIGNEUX, A., GARDIN, C., DELABESSE, E., SOULIER, J., HUNAULT, M., DOMBRET, H., ITZYKSON, R., CLAPPIER, E. and PREUDHOMME, C., 2023. UBTF tandem duplications define a distinct subtype of adult de novo acute myeloid leukemia. *Leukemia,* **37**(6), pp. 1245-1253.

DZAMA, M.M., STEINER, M., RAUSCH, J., SASCA, D., SCHÖNFELD, J., KUNZ, K., TAUBERT, M.C., MCGEEHAN, G.M., CHEN, C., MUPO, A., HÄHNEL, P., THEOBALD, M., KINDLER, T., KOCHE, R.P., VASSILIOU, G.S., ARMSTRONG, S.A. and KÜHN,

M.W.M., 2020. Synergistic targeting of FLT3 mutations in AML via combined menin-MLL and FLT3 inhibition. *Blood*, **136**(21), pp. 2442-2456.

FISKUS, W., MILL, C.P., BIRDWELL, C., DAVIS, J.A., DAS, K., BOETTCHER, S., KADIA, T.M., DINARDO, C.D., TAKAHASHI, K., LOGHAVI, S., SOTH, M.J., HEFFERNAN, T., MCGEEHAN, G.M., RUAN, X., SU, X., VAKOC, C.R., DAVER, N. and BHALLA, K.N., 2023. Targeting of epigenetic co-dependencies enhances anti-AML efficacy of Menin inhibitor in AML with MLL1-r or mutant NPM1. *Blood cancer journal (New York)*, **13**(1), pp. 53.

GUO, H., CHU, Y., WANG, L., CHEN, X., CHEN, Y., CHENG, H., ZHANG, L., ZHOU, Y., YANG, F., CHENG, T., XU, M., ZHANG, X., ZHOU, J. and YUAN, W., 2017. PBX3 is essential for leukemia stem cell maintenance in MLL-rearranged leukemia. *International journal of cancer*, **141**(2), pp. 324-335.

GUO, Z., SUN, L., XIA, H., TIAN, S., LIU, M., HOU, J., LI, J., LIN, H. and DU, G., 2022. Shikonin as a WT1 Inhibitor Promotes Promyeloid Leukemia Cell Differentiation. *Molecules (Basel, Switzerland)*, **27**(23), pp. 8264.

HOFFBRAND, A.V. and STEENSMA, D.P., 2020. *Hoffbrand's essential haematology*. Eighth edition edn. Chichester, UK: Wiley Blackwell.

ISSA, G.C., ALDOSS, I., DIPERSIO, J.F., CUGLIEVAN, B., STONE, R.M., ARELLANO, M.L., THIRMAN, M.J., PATEL, M.R., DICKENS, D., SHENOY, S., SHUKLA, N., ROSEN, G., BAGLEY, R.G., MEYERS, M.L., MADIGAN, K., ORDENTLICH, P., GU, Y., SMITH, S., MCGEEHAN, G.M. and STEIN, E., 2022. The Menin Inhibitor SNDX-5613 (revumenib) Leads to Durable Responses in Patients (Pts) with KMT2A-Rearranged or NPM1 Mutant AML: Updated Results of a Phase (Ph) 1 Study. *Blood*, **140**(Supplement 1), pp. 150-152.

ISSA, G.C., RAVANDI, F., DINARDO, C.D., JABBOUR, E., KANTARJIAN, H.M. and ANDREEFF, M., 2021. Therapeutic implications of menin inhibition in acute leukemias. *Leukemia*, **35**(9), pp. 2482-2495.

ITO, S., BARRETT, A.J., DUTRA, A., PAK, E., MINER, S., KEYVANFAR, K., HENSEL, N.F., REZVANI, K., MURANSKI, P., LIU, P., MELENHORST, J.J. and LAROCHELLE, A., 2015. Long term maintenance of myeloid leukemic stem cells cultured with unrelated human mesenchymal stromal cells. *Stem Cell Research*, **14**(1), pp. 95-104.

KABURAGI, T., SHIBA, N., YAMATO, G., YOSHIDA, K., TABUCHI, K., OHKI, K., ISHIKITA, E., HARA, Y., SHIRAISHI, Y., KAWASAKI, H., SOTOMATSU, M., TAKIZAWA, T., TAKI, T., KIYOKAWA, N., TOMIZAWA, D., HORIBE, K., MIYANO, S., TAGA, T., ADACHI, S., OGAWA, S. and HAYASHI, Y., 2023. UBTF-internal tandem duplication as a novel poor prognostic factor in pediatric acute myeloid leukemia. *Genes chromosomes & cancer,* **62**(4), pp. 202-209.

KAUR, G. and DUFOUR, J.M., 2012. Cell lines. *Spermatogenesis,* **2**(1), pp. 1-5.

KONOPLEVA, M., KONOPLEV, S., HU, W., ZARITSKEY, A.Y., AFANASIEV, B.V. and ANDREEFF, M., 2002. Stromal cells prevent apoptosis of AML cells by up-regulation of anti-apoptotic proteins. *Leukemia,* **16**(9), pp. 1713-1724.

KOSAN, C., GINTER, T., HEINZEL, T. and KRÄMER, O.H., 2013. STAT5 acetylation. *JAK-STAT,* **2**(4), pp. e26102.

LAGUNAS-RANGEL, F.A. and CHÁVEZ-VALENCIA, V., 2017. FLT3–ITD and its current role in acute myeloid leukaemia. *Medical oncology (Northwood, London, England),* **34**(6), pp. 114.

MATKAR, S., THIEL, A. and HUA, X., 2013. Menin: a scaffold protein that controls gene expression and cell signaling. *Trends in biochemical sciences (Amsterdam. Regular ed.),* **38**(8), pp. 394-402.

PERNER, F., STEIN, E.M., WENGE, D.V., SINGH, S., KIM, J., APAZIDIS, A., RAHNAMOUN, H., ANAND, D., MARINACCIO, C., HATTON, C., WEN, Y., STONE, R.M., SCHALLER, D., MOWLA, S., XIAO, W., GAMLEN, H.A., STONESTROM, A.J., PERSAUD, S., ENER, E., CUTLER, J.A., DOENCH, J.G., MCGEEHAN, G.M., VOLKAMER, A., CHODERA, J.D., NOWAK, R.P., FISCHER, E.S., LEVINE, R.L., ARMSTRONG, S.A. and CAI, S.F., 2023. MEN1 mutations mediate clinical resistance to menin inhibition. *Nature (London),* **615**(7954), pp. 913-919.

PISA, R. and KAPOOR, T.M., 2020. Chemical strategies to overcome resistance against targeted anticancer therapeutics. *Nature chemical biology,* **16**(8), pp. 817-825.

RASOULI, M., BLAIR, H., TROESTER, S., SZOLTYSEK, K., CAMERON, R., ASHTIANI, M., KRIPPNER-HEIDENREICH, A., GREBIEN, F., MCGEEHAN, G.,

ZWAAN, C.M. and HEIDENREICH, O., 2023. The MLL–Menin Interaction is a Therapeutic Vulnerability in NUP98-rearranged AML. *HemaSphere,* **7**(8),.

REYNOLDS, S., April 18, 2023-last update, Revumenib Shows Promise in Treating Advanced Acute Myeloid Leukemia. Available: https://www.cancer.gov/news-events/cancer-currents-blog/2023/revumenib-menin-inhibitor-advanced-aml [26/07/, 2023].

SLATS, A.M., EGELER, R.M., VAN DEN BERG, A., KORBIJN, C., HAHLEN, K., KAMPS, W.A., VEERMAN, A. and ZWAAN, C.M., 2005. Causes of death - other than progressive leukemia - in childhood acute lymphoblastic (ALL) and myeloid leukemia (AML): the Dutch Childhood Oncology Group experience. *Leukemia,* **19**(4), pp. 537-544.

SYAMA, K., HASSAN, E.M. and ZOU, S., 2021. Advances in culture methods for acute myeloid leukemia research. *Oncoscience,* **8**, pp. Oncoscience, Volume: 8, Publication date: 2021-04, Pages: 82–90.

TAKAHASHI, S., 2011. Downstream molecular pathways of FLT3 in the pathogenesis of acute myeloid leukemia: biology and therapeutic implications. *Journal of Hematology & Oncology,* **4**(1), pp. 13.

TAN, Z., KAN, C., WONG, M., SUN, M., LIU, Y., YANG, F., WANG, S. and ZHENG, H., 2022. Regulation of Malignant Myeloid Leukemia by Mesenchymal Stem Cells. *Frontiers in cell and developmental biology,* **10**, pp. 857045.

UMEDA, M., MA, J., HUANG, B.J., HAGIWARA, K., WESTOVER, T., ABDELHAMED, S., BARAJAS, J.M., THOMAS, M.E., WALSH, M.P., SONG, G., TIAN, L., LIU, Y., CHEN, X., KOLEKAR, P., TRAN, Q., FOY, S.G., MACIASZEK, J.L., KLEIST, A.B., LEONTI, A.R., JU, B., EASTON, J., WU, H., VALENTINE, V., VALENTINE, M.B., LIU, Y., RIES, R.E., SMITH, J.L., PARGANAS, E., IACOBUCCI, I., HILTENBRAND, R., MILLER, J., MYERS, J.R., RAMPERSAUD, E., RAHBARINIA, D., RUSCH, M., WU, G., INABA, H., WANG, Y., ALONZO, T.A., DOWNING, J.R., MULLIGHAN, C.G., POUNDS, S., BABU, M.M., ZHANG, J., RUBNITZ, J.E., MESHINCHI, S., MA, X. and KLCO, J.M., 2022. Integrated Genomic Analysis Identifies UBTF Tandem Duplications as a Recurrent Lesion in Pediatric Acute Myeloid Leukemia. *Blood cancer discovery,* **3**(3), pp. 194-207.

VAKITI, A. and MEWAWALLA, P., 2023. Acute Myeloid Leukemia. *StatPearls,* .

YOKOYAMA, A. and CLEARY, M.L., 2008. Menin Critically Links MLL Proteins with LEDGF on Cancer-Associated Target Genes. *Cancer Cell*, **14**(1), pp. 36-46.

YOKOYAMA, A., SOMERVAILLE, T.C.P., SMITH, K.S., ROZENBLATT-ROSEN, O., MEYERSON, M. and CLEARY, M.L., 2005. The Menin Tumor Suppressor Protein Is an Essential Oncogenic Cofactor for MLL-Associated Leukemogenesis. *Cell*, **123**(2), pp. 207-218.